Bachelor Thesis

Theoretic Acousto-fluidics in Microsystems

Sofie Sabine Rose Moth s042251

Julie Refsgaard Lawaetz s042499

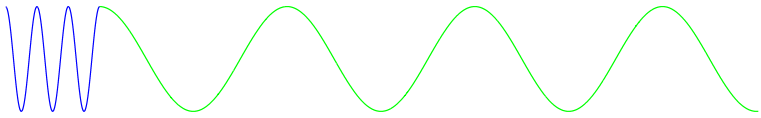

Supervisor: Henrik Bruus

MIC – Department of Micro and Nanotechnology
Technical University of Denmark

19 June 2007

Abstract

Recent research in acousto-fluidics has shown useful results within the area of the lab-on-a-chip-technology. Applying an acoustic field to a microfluidic system give rise to the acoustic radiation force and acoustic streaming. Both phenomena find great use within separation or mixing of particles contained in a liquid within biomedical areas. Knowledge of resonance is a precondition in order to make use of acousto-fluidics to flow control.

Using perturbation theory this thesis emphasis the understanding of the resonance case rising from the first order acoustic field. Resonance conditions have been studied in different simple designs of micro systems primarily with the inclusion of attenuation.

The overall findings of the project indicate the case of resonance to depend on the acoustic material parameters as well as the setup and geometry of the system.

Preface

This bachelor thesis treats the theory of acousto-fluidics in micro systems with particular emphasis on acoustic resonance phenomena. Acoustic fields are derived using perturbation theory.

The thesis covers the effort of 15 ETCS points corresponding to half a semester workload and has been prepared in the spring semester 2007 at Department of Micro and Nanotechnology (MIC), DTU.

During the work with this project we have appreciated the help of personnel from MIC. We would especially like to thank our supervisor Henrik Bruus for giving support and providing the requisite advising, and Peder Skafte-Pedersen for being a great help with different aspects concerning the theory.

Julie Refsgaard Lawaetz s042499 and Sofie Sabine Rose Moth s042251
MIC – Department of Micro and Nanotechnology
Technical University of Denmark
19 June 2007

Contents

List of Figures

List of Tables

List of symbols

Symbol	Description	Unit
$\boldsymbol{v}$	Velocity vector	m s^{-1}
$\boldsymbol{g}$	Gravity	N kg^{-1}
$\mathbf{F}$	Acoustic radiation force	N
Z_j	Characteristic impedance	kg m^{-2} s^{-1}
$\phi(r,t)$	Velocity potential	m^2 s^{-1}
v	Velocity	m s^{-1}
p	Pressure	N m^{-2}
T	Temperature	K
L	Length of system	m
ρ	Mass density	kg m^{-3}
ℓ	Amplitude of vibrating wall	m
ω	Angular frequency	s^{-1}
f	Frequency	Hz
k	Wave number	m^{-1}
η	Viscosity	Pa s
c_a	Speed of sound	m s^{-1}
$\mathbf{e}_r$	Unit vector in r direction	
$\mathbf{e}_\theta$	Unit vector in θ direction	
i	Imaginary unit	
γ	Damping parameter	

Chapter 1

Introduction

In recent years lab-on-a-chip technology has been found to be an important research area with many applications. All investigations are rather new and therefore more knowledge about it is needed. Acousto-fluidics is one important component that is not yet been completely described.

In this thesis the theory providing acoustics in microfluidic systems is investigated with the aim to deliver a thoroughly description of resonance in simple geometrical cases.

Acousto-fluidics is the study of longitudinal waves propagating in microfluidic systems. In order to let waves into the fluid it must be treated as compressible. The acoustic field is activated by a piezo actuator which in the selected models is placed at different boundaries.

Two kind of designs are considered applying various boundary conditions and extending from one to two domains.

Chapter 2

Basic theory of acoustic microfluidics

2.1 Lab-on-a-chip

A laboratory installed on a chip is now possible and is implemented by the lab-on-a-chip technology. Acoustic microfluidics find great utilization within lab-on-a-chip systems. The research area has undergone a great development since the early 1990ies. Having laboratories with sample channels on the 100 μm scale present a lot of advantages compared to normal size laboratories. A smaller amount of sample is preferable, e.g., if the sample is expensive or limited in size. The small amount of sample also leads to shorter diffusion times due to smaller distances. Furthermore the lab-on-a-chip device is transportable and has potential to be low-cost mass produced. Lab-on-a-chip systems are expected to have potential within the fields of analyzing various samples especially areas of medical diagnosis, biotechnology, environmental measurements. Only a droplet of blood from a patient is enough to establish a full diagnose in a few minutes; salmonella can be detected directly in the slaughterhouse and the field working biologists are able to analyze a sample of sea water on location.

However the small length scale influences the physical properties of the system. Dealing with microfluidics the surface of a given particle becomes large compared to the volume of the particle. Compared to the surface-volume-ratio occurring in macro-fluidics this ratio is significantly changed. This implies that surface forces, such as tension and viscosity, dominates body forces, i.a., gravity, inertia.

2.2 Describing a fluid

A fluid is characterized by having no preferred shape in contrast to a solid. Even small shear forces induce large changes in the relative positions of the fluid elements whereas in a solid similar forces induce only small changes in the relative positions of the elements. When no longer influenced by external forces the fluid does not necessarily retract to its initial shape unlike a solid.

There are two classes of fluids: gasses and liquids. The main difference between a gas and a liquid concerns the density and the degree of interaction between the molecules of the fluid. An ideal gas has the density $\rho_{\text{gas}} \approx 1$ kg m^{-3} allowing the constituent molecules to move almost as free particles. Due to the relatively large average intermolecular distance, approximately 3 nm, a gas is compressible. In contrast a liquid has the density $\rho_{\text{liq}} \simeq 10^3$ kg m^{-3} at 1 atm and 300 K similar to the density of a solid. The molecules are thus densely packed with an average intermolecular distance of approximately 0.3 nm and a liquid may for low liquid velocities be considered incompressible. However, the focus in this report is acousto-fluidics where compressibility of the fluid do play a role, further examination in section 2.2.1.

The length scale of a lab-on-a-chip system is typically 10 μm $-$ 100 μm. Given the length scale of the intermolecular distances for fluids, 3 nm and 0.3 nm for gasses and liquids, respectively, the fluid in a lab-on-a-chip system can be considered as a continuum. The thermal fluctuations in small volumes averages close to zero and influence from the individual molecules is thus insignificant. The fluid can therefore be considered as continuous implying properties such as density, pressure, temperature, and velocity to be assumed as well defined in every point of the fluid, [11]. The fluid can now be described by fluid particles; small regions containing enough molecules for the continuum hypothesis to hold and yet small enough for no external forces to change the physical properties of the fluid within the fluid particle. This implies that a fluid particle does not have a definite volume, though the side length of a cubic fluid particle is approximately 10 nm. It is therefore advantageous to define the governing equations per volume in fluidics.

Having fixed geometry in the system it is common to use the Eulerian description where the flow is considered at fixed points $\mathbf{r}$ for all time t, i.e., $\mathbf{r}$ is independent of t. An alternative is the Lagrangian description involving changing position vector $\mathbf{r}(t)$ of a fluid particle, i.e., $\mathbf{r}$ is dependent of t.

2.2.1 Acousto-fluidics

Acousto-fluidics is the study of longitudinal waves propagating in microfluidic systems and the fluid must be treated as compressible. The acoustic field can be created by an AC biased piezo-actuator externally or internally by implementing the piezo-actuator in the chip. The frequency of the actuator determines the wavelengths of the acoustic fields. These must necessarily be less than the order magnitude of the lab-on-a-chip system, i.e., $\lambda \leq 10^{-3}$ m. Based on this size of wavelength frequency is set to $f \approx 10^6$ Hz rendering the possibility of resonance phenomena to occur in the micro-system.

The sound velocity in water is $c_{\text{w}} \simeq 1.42 \times 10^3$ m s^{-1} whereas the sound velocity in air is $c_{\text{air}} \simeq 3.4 \times 10^2$ m s^{-1}.

Since the sound velocity in liquids is given by the isentropic pressure derivative with respect to the density the sound velocity can not be interpreted as being constant. This

is a consequence of operating with compressible liquids, i.e, liquids with varying densities. However when applying perturbation theory this only becomes of importance in the second order expansion, see section 2.4.

2.3 Fundamental equations

In order to characterize a moving fluid only the velocity field $\mathbf{v}(\mathbf{r}, t)$, the pressure field $p(\mathbf{r}, t)$ and the density field $\rho(\mathbf{r}, t)$ are needed; the latter two are thermodynamic variables and others may be used, e.g., the temperature field $T(\mathbf{r}, t)$. To determine these properties, the continuity equation, the Navier–Stokes equation and the heat equation are utilized. These three governing equations are all conservation laws stating conservation of mass, momentum and energy, respectively, and will be described in the following sections.

2.3.1 The continuity equation

The continuity equation Eq. (2.1) stating mass conservation is given by

$$\partial_t \rho \quad = \quad -\boldsymbol{\nabla} \cdot (\rho \mathbf{v}). \tag{2.1}$$

Expressing mass conservation per volume has the advantage that knowing the volume of the treated system is not necessary.

It is noted that if the flow velocity is significantly smaller than the sound velocity, the fluid may be considered incompressible, i.e., ρ is constant. This results in $\boldsymbol{\nabla} \cdot \mathbf{v} = \mathbf{0}$ for incompressible fluids, cf. Eq. (2.1).

2.3.2 The Navier–Stokes equation

The Navier–Stokes equation states momentum conservation and is the equation of motion for fluids corresponding to Newton's second law for particles expressing force per volume. Neglecting gravitational force and electrical force but keeping the forces caused by pressure and viscosity, the Navier–Stokes equation reads

$$\rho\Big(\partial_t \mathbf{v} + (\mathbf{v} \cdot \boldsymbol{\nabla})\mathbf{v}\Big) = -\boldsymbol{\nabla} p + \eta \nabla^2 \mathbf{v} + \beta\eta \boldsymbol{\nabla}(\boldsymbol{\nabla} \cdot \mathbf{v}), \tag{2.2}$$

where η denotes the dynamic viscosity due to inner friction during shear, here assumed to be constant, and β is a numerical constant of order unity for simple fluids, $\beta \simeq \frac{5}{3}$, related to the second viscosity caused by internal friction during compression. It arises when there are non-zero velocity gradients within the fluid. In the case of an incompressible fluid the term containing β is zero due to $\boldsymbol{\nabla} \cdot \mathbf{v} = \mathbf{0}$

On the left-hand side of Eq. (2.2) is given the acceleration in as the time derivative of the velocity. Because of the usage of Eulerian notation the material time-derivative $D_t = \partial_t + (\mathbf{v} \cdot \boldsymbol{\nabla})$ is applied. On the right-hand side are force contributions due to pressure and viscosity. Regarding the whole equation the pressure p is seen to be the source term giving rise to a change in velocity.

2.3.3 The heat transfer equation

The heat transfer equation stating conservation of energy for a fluid is the third and last governing equation. It is derived using the first fundamental law of thermodynamics and concerns the conduction of convection of heat within a fluid. However considerations of heat evolution in microfluidic systems is beyond the scope of this project. The heat transfer equation will therefore not be further described.

2.4 Perturbation theory

Due to nonlinearity the governing equations for fluidics are difficult – and often impossible – to solve analytically. However by adding a small perturbation to a problem with an already known solution, denoted the zeroth order solution, it is possible to approximate a solution to the perturbed system. This method of determining an approximate solution to an otherwise analytically unsolvable problem is known as perturbation theory.

Most acoustics phenomena can be treated as relatively small perturbations to the static case and by the use of first and second order perturbation theory acoustic fields and effects will be described in microfluidic systems.

2.4.1 First order - the acoustic wave equation

In acoustics the wave equation cannot be derived as an exact equation. However applying the method of first order perturbation, and combining the governing equations are found to entail the well known wave equation, which applies for the three physical properties pressure, density and velocity. The wave equation is thus an approximation based on the combination of the thermodynamic equation of state, the continuity equation and the Navier–Stokes equation summarized here

$$p = p(\rho), \tag{2.3}$$
$$\partial_t \rho = -\boldsymbol{\nabla} \cdot (\rho \mathbf{v}), \tag{2.4}$$
$$\rho \partial_t \mathbf{v} = -\boldsymbol{\nabla} p - \rho(\mathbf{v} \cdot \boldsymbol{\nabla})\mathbf{v} + \eta \nabla^2 \mathbf{v} + \beta\eta \boldsymbol{\nabla}(\boldsymbol{\nabla} \cdot \mathbf{v}). \tag{2.5}$$

A small perturbation is added to the constant zeroth order terms for the pressure p_0, density ρ_0 and velocity field $\mathbf{v}_0$. The liquid is assumed to be at rest before applying the acoustic field, i.e., $\mathbf{v}_0 = \mathbf{0}$. Hence with the perturbation of first order the pressure, density and velocity are defined as

$$p = p_0 + p_1, \tag{2.6a}$$
$$\rho = \rho_0 + \rho_1, \tag{2.6b}$$
$$\mathbf{v} = \mathbf{0} + \mathbf{v}_1. \tag{2.6c}$$

Inserting the perturbation in Eqs. (2.3), (2.4), and (2.5) and linearizing, i.e, disregarding terms of higher order where the sum of indices in a given term exceeds 1, the following is

obtained neglecting viscosity

$$p_1 = c_a^2 \rho_1, \tag{2.7a}$$
$$\partial_t \rho_1 = -\rho_0 \boldsymbol{\nabla} \cdot \mathbf{v}_1, \tag{2.7b}$$
$$\rho_0 \partial_t \mathbf{v}_1 = -\boldsymbol{\nabla} p_1 = -c_a^2 \boldsymbol{\nabla} \rho_1, \tag{2.7c}$$

where Eq. (2.7a) is obtained by a Taylor expansion around ρ_0 and the definition of the sound velocity

$$c_a^2 \equiv \left(\partial_\rho p\right)_0 = \left(\frac{\partial p}{\partial \rho}\right)_s. \tag{2.8}$$

The subscript s denotes the pressure derivative being isentropic. Note that terms containing $\mathbf{v}_0$ do not appear in Eq. (2.7) because the starting point is the static case and derivatives of ρ_0 are zero.

Sound velocity

The sound velocity is calculated by the pressure derivative with respect to the density. Having constant sound velocity implies a linear relation between the pressure and the density. However this does not seem to be our case. Determining the linearity of the pressure versus density the following ratio of the first and second derivatives are considered

$$\gamma^* - 1 = \frac{\rho_0 (\partial_\rho^2 p)_0}{(\partial_\rho p)_0} = \frac{\rho_0 \partial_\rho (c_a^2)}{c_a^2}. \tag{2.9}$$

$\gamma^* - 1$ is known as the non-linear parameter of the media, [2]. In order to simplify the calculations by assuming the sound velocity to be constant this parameter must be zero. However, referring to the data for water given by [5], cf. App. A.1, the sound velocity cannot be assumed to be constant since an estimation of the parameter gives $\gamma^* - 1 \approx 6$. For ideal gasses the nonlinear parameter is $\frac{7}{5} - 1 = \frac{2}{5}$. Expecting fluids to be more linear than gasses the estimation $\gamma^* - 1 \approx 6$ for water is not good. However the estimation is based on only four values of pressure and corresponding density and moreover three of these concern pressures above 1 MPa. This is too high compared to the pressure present in lab-on-a-chip systems being approximately 1 atm = 0.1 MPa. Referring to the data given by [5], the sound velocity cannot be assumed to be constant. A method to determine the parameter $\gamma^* - 1$ has been given, but more suitable data of pressure-density around 0.1 MPa is needed to make further conclusions.

However this parameter only appears in the second order perturbation. In first order perturbation the derivative $(\partial_\rho^2 p)_0$ do not occur which leads to $\gamma^* - 1 = 0$, i.e, the velocity is constant to first order perturbation but can not be assumed constant to second order. We shall see that the non-linear parameter is of importance in acoustic streaming and radiation force since these stems from the second order perturbation, more about these phenomenons in section 2.4.2.

The acoustic wave equation

The Eqs. (2.7) can now be used to derive the wave equations for p_1, ρ_1 and $\mathbf{v}_1$. Starting with ρ_1 the divergence of Eq. (2.7c) is taken

$$\rho_0 \boldsymbol{\nabla} \cdot (\partial_t \mathbf{v}_1) = -c_a^2 \nabla^2 \rho_1. \tag{2.10}$$

Using that ∂_t and $\boldsymbol{\nabla}$ commute and $\boldsymbol{\nabla} \cdot (\boldsymbol{\nabla} \cdot \mathbf{v}) = \nabla^2 \mathbf{v} + \boldsymbol{\nabla} \times \boldsymbol{\nabla} \times \mathbf{v} = \nabla^2 \mathbf{v}$ since $\mathbf{v}$ is a gradient field and thus $\boldsymbol{\nabla} \times \mathbf{v} = \mathbf{0}$, followed by insertion of Eq. (2.7b) the wave equation for ρ_1 reads

$$\partial_t^2 \rho_1 = c_a^2 \nabla^2 \rho_1. \tag{2.11}$$

The wave equation for $\mathbf{v}_1$ is likewise obtained by computing the gradient of Eq. (2.7b), making use of the previous mentioned relation and inserting Eq. (2.7c)

$$\partial_t^2 \mathbf{v}_1 = c_a^2 \nabla^2 \mathbf{v}_1. \tag{2.12}$$

From the proportionality relation between p_1 and ρ_1, cf. Eq. (2.7a), the wave equation for p_1 is easily obtained by dividing the wave equation for ρ_1, Eq. (2.11), by c_a^2,

$$\partial_t^2 p_1 = c_a^2 \nabla^2 p_1. \tag{2.13}$$

The velocity potential

The wave equations for ρ_1, p_1 and $\mathbf{v}_1$ are obtained by assuming negligible viscosity. The three acoustic fields are thus found to obey the same wave equation in the non-viscous case. By introducing the velocity potential $\phi_1(\mathbf{r}, t)$ defined by

$$\mathbf{v}_1 = \boldsymbol{\nabla} \phi_1 \tag{2.14}$$

and using Eqs. (2.7), the first order terms for p_1 and ρ_1 yields

$$p_1 = -\rho_0 \partial_t \phi_1, \tag{2.15}$$

$$\rho_1 = \frac{-\rho_0}{c_a^2} \partial_t \phi_1. \tag{2.16}$$

All fields can thus be obtained from

$$\partial_t^2 \phi = c_a^2 \nabla^2 \phi. \tag{2.17}$$

One solution to this differential equation is the harmonic plane wave propagating along the wave vector $\mathbf{k}_0 = k_0 \mathbf{e}_{k_0}$ with the constant amplitude ϕ_0 and the angular frequency $\omega = 2\pi f$,

$$\phi(\mathbf{r}, t) = \phi_0 e^{i(\mathbf{k}_0 \cdot \mathbf{r} - \omega t)}, \tag{2.18}$$

where $k_0 = \frac{\omega}{c_a} = \frac{2\pi}{\lambda}$ is the wave number.

Another solution to Eq. (2.17) is the standing wave with the position and wavelength dependent amplitude $\phi_{k_0}(\mathbf{r})$

$$\phi(\mathbf{r},t) = \phi_{k_0}(\mathbf{r})e^{-i\omega t}. \tag{2.19}$$

Inserting the standing wave in the wave equation results in the Helmholtz equation

$$\nabla^2\phi_{k_0}(\mathbf{r}) = -\frac{\omega^2}{c_a^2}\phi_{k_0}(\mathbf{r}) = -k_0^2\phi_{k_0}(\mathbf{r}). \tag{2.20}$$

The Helmholtz equation is an eigenvalue equation which gives specific eigenvalues of k_0 and corresponding eigenmodes $\phi_{k_0}(\mathbf{r})$, also called resonance modes, when solved using homogenous boundary conditions.

The viscous case

Concerning acoustic waves in a liquid damping is a consequence of the friction arising when waves propagate through the liquid. Taking into account the attenuation of the acoustic waves the viscosity can no more be neglected and the first-order part of the Navier–Stokes equation (2.5) becomes

$$\rho_0\partial_t\mathbf{v}_1 = -c_a^2\boldsymbol{\nabla}\rho_1 + \eta\nabla^2\mathbf{v}_1 + \beta\eta\boldsymbol{\nabla}(\boldsymbol{\nabla}\cdot\mathbf{v}_1). \tag{2.21}$$

To determine the modified wave equation of ρ_1 with viscous damping the divergence of Eq. (2.21) is calculated

$$\rho_0\partial_t\boldsymbol{\nabla}\cdot\mathbf{v}_1 = -c_a^2\nabla^2\rho_1 + (1+\beta)\eta\nabla^2(\boldsymbol{\nabla}\cdot\mathbf{v}_1). \tag{2.22}$$

Inserting Eq. (2.7b) leads to

$$\partial_t^2\rho_1 = c_a^2\nabla^2\rho_1 + \frac{(1+\beta)\eta}{\rho_0}\nabla^2(\partial_t\rho_1). \tag{2.23}$$

To solve this wave equation a harmonically varying time-dependent function, $\rho_1(t) = Ae^{-i\omega t}$ where A is an arbitrary constant, provides a good guess of the solution. This results in the Helmholtz equation with a complex prefactor instead of k_0^2 as in Eq. (2.20)

$$-\omega^2\rho_1 = c_a^2\Big[1 - i2\gamma\Big]\nabla^2\rho_1, \tag{2.24}$$

$$\gamma = \frac{(1+\beta)\eta\omega}{2\rho_0 c_a^2} \approx \frac{10^{-3}\ \text{Pa s} \times 10^6\ \text{s}^{-1}}{10^3\ \text{kg m}^{-3} \times (10^3\ \text{m s}^{-1})^2} = 10^{-6} \ll 1. \tag{2.25}$$

Due to the small value of γ the approximation $1 - i2\gamma \simeq (1+i\gamma)^{-2}$ is quite precise. Isolating $\nabla^2\rho_1$ from Eq. (2.24) and using the Taylor expansion of the complex prefactor the modified Helmholtz equation equivalent to Eq. (2.20) is obtained

$$\nabla^2\rho_1 = -\frac{\omega^2}{c_a^2}\Big[1 + i\gamma\Big]^2\rho_1 = -k^2\rho_1, \tag{2.26}$$

where

$$k = k_0(1 + i\gamma). \tag{2.27}$$

The modified Helmholtz equation for ϕ_1 including attenuation is derived using Eqs. (2.16)

$$\nabla^2\phi_1 = -k^2\phi_1, \tag{2.28}$$

k given by Eq. (eq:k). Taking the gradient of Eq. (2.28) results in the modified Helmholtz equation for $\mathbf{v}_1$

$$\nabla^2\mathbf{v}_1 = -k^2\mathbf{v}_1, \tag{2.29}$$

k given by Eq. (eq:k). The damping is due to the imaginary part of Eq. (2.30) and to estimate the magnitude of the damping k_0 and $k_0\gamma$ is calculated,

$$k_0 = \frac{\omega}{c_a} \approx \frac{10^6\ \mathrm{s}^{-1}}{10^3\ \mathrm{m\ s}^{-1}} \approx 10^3\ \mathrm{m}^{-1}, \quad k_0\gamma \approx 10^3\ \mathrm{m}^{-1} \times 10^{-6}\ \approx 10^{-3}\ \mathrm{m}^{-1}. \tag{2.30}$$

The value of $k_0\gamma$ is minute but in some case of resonance the damping will be of huge importance if appearing in the denominator of an amplitude. This is studied in the further chapters.

2.4.2 Second order perturbation - time averaging

Assuming harmonic time-dependency the factor $e^{-i\omega t}$ is contained within all terms of the first order expansion. This leads to no DC drift velocity because the harmonic factor $e^{-i\omega t}$ has the real part $\cos(\omega t)$ and therefore the time average equals zero over a full period. However expanding to second order gives rise to terms containing products of the two factors $\mathrm{Re}(e^{-i\omega t})$ due to the non-linearity of the continuity equation and Navier–Stokes equation. Using $\langle A(t)B(t)\rangle = \frac{1}{2}\mathrm{Re}[A_0B_0^*]$, see App. B, this product is found to have the time average $\frac{1}{2}$ over a full period. This result is likewise found by regarding the product of the two real parts of the factor, $\cos^2(\omega t)$, which has the full-period-time average $\frac{1}{2}$. In contrast to first order DC drift velocity is therefore present when including second order terms. The second order expansion reads

$$p = p_0 + p_1 + p_2, \tag{2.31a}$$
$$\rho = \rho_0 + \rho_1 + \rho_2, \tag{2.31b}$$
$$\mathbf{v} = \mathbf{0} + \mathbf{v}_1 + \mathbf{v}_2. \tag{2.31c}$$

As for first order the liquid is assumed to be at rest before applying the acoustic field, i.e., $\mathbf{v}_0 = \mathbf{0}$. Combining Eqs. (2.3), (2.4), (2.5) and (2.31) gives

$$p_2 = {c_a}^2\rho_2 + \tfrac{1}{2}(\partial_\rho c^2)_0\rho_1^2 = c_a^2\rho_2 + \frac{\gamma^* - 1}{2}\frac{c_a^2}{\rho_0}\rho_1^2, \tag{2.32a}$$
$$\partial_t\rho_2 = -\rho_0\boldsymbol{\nabla}\cdot\mathbf{v}_2 - \boldsymbol{\nabla}\cdot(\rho_1\mathbf{v}_1), \tag{2.32b}$$
$$\rho_0\partial_t\mathbf{v}_2 = -\rho_1\partial_t\mathbf{v}_1 - \rho_0(\mathbf{v}_1\cdot\boldsymbol{\nabla})\mathbf{v}_1 - c_a^2\boldsymbol{\nabla}\rho_2 - \tfrac{1}{2}\boldsymbol{\nabla}(\partial_\rho c_a^2)\rho_1^2 + \eta\nabla^2\mathbf{v}_2 + \beta\eta\boldsymbol{\nabla}(\boldsymbol{\nabla}\cdot\mathbf{v}_2). \tag{2.32c}$$

A Taylor expansion of p_2 around ρ_0 is used to obtain Eq. (2.32a) recalling the definition $c_a^2 \equiv (\frac{\partial p}{\partial \rho})_s$. The remaining procedure is analogue to the approach of first order expansion, i.e., all terms of higher order than two are excluded.

Acoustic radiation force

A body contained within a fluid subject to an acoustic field is influenced by the acoustic radiation pressure force denoted $\mathbf{F}$. Assuming the body is elastic with the time-dependent surface $S(t)$ the time average of the acoustic radiation force $\mathbf{F}$ acting on the body is given by

$$\langle \mathbf{F} \rangle = -\rho_0 \Big\langle \int_{S_0} \mathrm{d}a \, (\mathbf{n} \cdot \boldsymbol{\nabla}\phi_1) \boldsymbol{\nabla}\phi_1 \Big\rangle - \frac{\rho_0}{2c_a^2} \Big\langle \int_{S_0} \mathrm{d}a \, \mathbf{n} \big(\partial_t \phi\big)^2 \Big\rangle + \frac{\rho_0}{2} \Big\langle \int_{S_0} \mathrm{d}a \, \mathbf{n} |\boldsymbol{\nabla}\phi_1|^2 \Big\rangle, \tag{2.33}$$

where $\boldsymbol{\nabla}\phi_1 = \mathbf{v}_1$ and $\partial_t \phi_1 = -\frac{p_1}{\rho_0}$. The middle term represents the potential energy whereas the last represents the kinetic energy. A specific name of energy cannot be assigned to the first term, but still it can be established that all three terms stem from a pressure force. The radiation force scales with the volume of the particle upon which it acts, [9]. Note that the surface variation $S(t)$ is replaced in all terms by the constant surface S_0 being the equilibrium position. This is allowed since the surface variation can be presumed as a perturbation, i.e., $S(t) = S_0 + \delta S(t)$. Including time dependency will expand the expression (2.33) to third order but when only operating with second order the time dependency must be discarded.

Acoustic streaming

The DC velocity time-independent component, resulting from the inclusion of second order terms, is known as acoustic streaming. The time-average of Eq. (2.32b) is determined to

$$\boldsymbol{\nabla} \cdot \langle \mathbf{v}_2 \rangle = -\frac{1}{\rho_0} \boldsymbol{\nabla} \cdot \langle \rho_1 \mathbf{v}_1 \rangle, \tag{2.34}$$

because $\langle \partial_t \rho_2 \rangle$ equals zero. Furthermore the time-average of Eq. (2.32c) is derived by taking the divergence and inserting Eq. (2.34)

$$\nabla^2 \langle \rho_2 \rangle = -\frac{1}{2c_a^2} (\partial_\rho c^2)_0 \nabla^2 \langle \rho_1^2 \rangle - \frac{\rho_0}{c_a^2} \boldsymbol{\nabla} \cdot \langle (\mathbf{v}_1 \cdot \boldsymbol{\nabla}) \mathbf{v}_1 \rangle + \frac{i\omega}{c_a^2} \boldsymbol{\nabla} \cdot \langle (\rho_1 \mathbf{v}_1) \rangle - \frac{\eta(\beta+1)}{\rho_0 c_a^2} \nabla^2 (\boldsymbol{\nabla} \cdot \langle \rho_1 \mathbf{v}_1 \rangle). \tag{2.35}$$

In appendix C a more detailed derivation of Eqs. (2.34) and (2.35) can be found.

Chapter 3

Background and motivation

3.1 Research done by MIC groups and others

Different groups at MIC have studied phenomena in lab-on-a-chip systems using acoustic waves to mix or trap the particles within the liquid in a chamber. Visual inspections of the waves have been carried out and compared with numerical results. The experiments have been observed to be qualitatively in accordance with the simulations and thus validating the theory.

However more investigation of the subject is needed and many areas are currently not clear. A suitable design of the system, resonance cases, thermal effects etc. are still subject to further studies.

We have read various articles dealing with the biomedical use of acoustic waves in micro systems. These are discussed in section 6. On the basis of these investigations the theory provided in this report is applied in selected geometrical configurations with the issue of resonance created by a piezo actuator of particular interest. Beginning with a simple one-dimensional system with one domain and no damping we extend the model to a two-dimensional system consisting of two domains with damping.

3.2 Physical assumptions and considerations

A number of assumptions and simplifications are made in order to set up a rather simple mathematical model of the regarded systems. We consider only steady state cases with no external forces acting in addition to the influence of the piezo actuator. The pressure is assumed to be small in order to maintain a laminar flow, hereby avoiding complex turbulent flow. The temperature is set to be within a range useful for biomedical research, e.g., around $T = 300$ K.

The frequency at which the piezo actuator vibrates is ultrasonic, i.e., about one MHz. Until now it has only been possible to measure the amplitude, ℓ, of vibrations induced by the piezo actuator in vacuum to the value $\ell = 10^{-9}$ m. However this amplitude may

be considerably smaller when the piezo actuator is vibrating against a layer of e.g. air, water or silicon. The specific amplitude of the damped vibration is not yet determined experimentally to the best of our knowledge. The amplitude is therefore unknown and can be chosen rather freely in order to create a realistic set up for the system. This implies ℓ to be considered as a fitting constant of the system and in this report we shall use $\ell = 10^{-10}$ m. For simplicity we assume the piezo actuator to be in direct contact with the regarded micro-systems, in contrast to the general experimental setup where there may be layers in between. A description of the physics of the piezo-actuator is not within the aim of this report and will therefore not be treated further.

3.3 Used parameters of the systems

The parameters used in the different systems are listed below in table 3.1.

Parameter	Value	Description
ℓ	1×10^{-10} m	Amplitude of the vibration
f	1×10^{6} Hz	Frequency (*)
ω	$2\pi \times 10^{6}$ s^{-1}	Angular frequency (*)
ρ_{w}	1.0×10^{3} kg m^{-3}	Density of water
ρ_{Si}	2.3×10^{3} kg m^{-3}	Density of silicon
$\langle c_{\mathrm{w}} \rangle$	1.42×10^{3} m s^{-1}	Sound velocity in water
$\langle c_{\mathrm{Si}} \rangle$	8.5×10^{3} m s^{-1}	Sound velocity in silicon

Table 3.1: Parameters of the systems [1]. (*) The values of the frequency and the angular frequency may be variable in some of the considered systems depending on the given boundary conditions.

3.4 Introduction to the systems

Using first order perturbation we consider variants of microfluidic systems containing mainly water. Starting with the simple case of a cross-section of one domain between two vibrating walls we next consider a cross-section of two domains activated by a piezo actuator placed at one of the walls. Hereinafter we expand the system to two dimensions by regarding systems consisting of a circular domain is investigated followed by two models of two concentric circular domains with different boundary conditions.

The models are simplified and idealized with the purpose of studying resonance phenomena. The emphasis is on the derivation of solutions and not on computing exact values of various fields. Thus the findings provided by the studied models are limited to indicate tendencies in preference to provide accurate values. However still the models overall contribute to the understanding of how and when resonance occurs in microfluidic systems.

Chapter 4

One dimensional micro systems

To study acoustic resonance in comparatively simple models the one dimensional system consisting of one domain comprising water is investigated applying two piezo actuators at each boundary of the system. Having the resonance cases in preference these are studied both in the viscous and non-viscous cases. As an extension of the first system a two domain model is hereinafter considered where the second domain constitutes of silicon. The boundary condition of this domain is an absorbing wall.

Using different boundary conditions general solutions to the given systems are derived and compared to experimental work done by others.

For each of the two models a figure shows the sketch of the systems with boundary conditions inscribed.

4.1 One domain enclosed by two piezo actuators

We wish to determine the acoustic fields of first order in a system consisting of two vibrating walls. The walls are parallel to the yz-plane and placed at $x = 0$ and $x = L$, where $L = 1$ mm. The walls vibrate with the frequency $f = 10^6$ s^{-1}, i.e, $\omega = 2\pi \times 10^6$ s^{-1}, and the amplitude of the vibration is $\ell = 10^{-10}$ m. The two walls imply two phase shifted waves generating a velocity field of the size $v = \omega\ell = 10^{-4}$ ms^{-1} in the vicinity of the walls. The system is sketched in Fig. 4.1.

Using first order perturbation and assuming $\mathbf{v}_0 = \mathbf{0}$, we have $\mathbf{v} = \mathbf{v}_1$. The wave equation for the velocity including damping and assuming harmonic time-dependency, cf. Eq. (2.29), is in one dimension given by

$$\partial_x^2 v_1 = -k^2 v_1, \tag{4.1}$$

where $k = k_0(1 + i\gamma)$. We study resonance in the case of two walls vibrating in opposite phase and the boundary conditions for the velocity field are

$$v(0, t) = \omega\ell e^{-i\omega t}, \tag{4.2a}$$

$$v(L, t) = -v(0, t). \tag{4.2b}$$

We recall that a simple solution to the wave equation, Eq. (4.1), is the harmonic plane wave

$$v(x,t) = (Ae^{ikx} + Be^{-ikx})e^{-i\omega t}, \qquad 0 < x < L, \tag{4.3}$$

where $\gamma \simeq 10^{-6}$, cf. Eq. (2.25). Solutions containing $e^{i\omega t}$ are discarded due to the given boundary conditions.

Regarding the case where k is real, i.e., no attenuation, the constants A and B are determined using Eqs. (4.2a), (4.2b) and (4.3)

$$A = \frac{\omega\ell}{2}\left(1 - i\frac{\cos(k_0 L) + 1}{\sin(k_0 L)}\right), \tag{4.4}$$

$$B = \frac{\omega\ell}{2}\left(1 + i\frac{\cos(k_0 L) + 1}{\sin(k_0 L)}\right). \tag{4.5}$$

Since the constants are determined by a sine function in the denominator they diverge for $k_0 = \frac{n\pi}{L}$, for $n = 1, 2, 3....$ The consequence is a resonance of infinite amplitude.

However the system contains water and damping is therefore present due to viscosity. The wave number k is therefore not real and the constants read

$$A = \frac{\omega\ell}{2}\left(1 - i\frac{\cos(kL) + 1}{\sin(kL)}\right), \tag{4.6}$$

$$B = \frac{\omega\ell}{2}\left(1 + i\frac{\cos(kL) + 1}{\sin(kL)}\right). \tag{4.7}$$

$$\tag{4.8}$$

As in the real case resonance occurs in the system when the sine function in the denominator of the second term has minima. Using Taylor expansion around $k_0 L$ the denominator reads

$$\sin(kL) = \sin\big(k_0(1 + i\gamma)L\big), \tag{4.9}$$

$$\simeq \sin(k_0 L) + i\gamma k_0 L\cos(k_0 L). \tag{4.10}$$

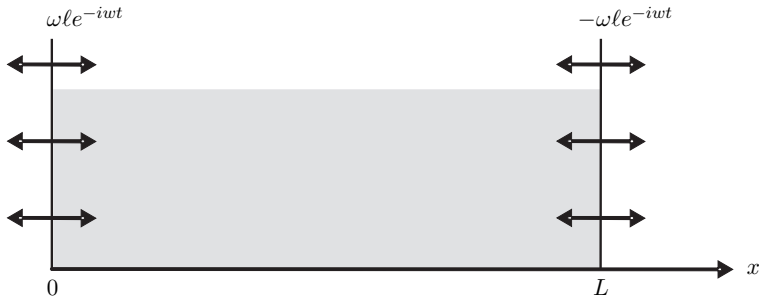

Figure 4.1: A sketch of the microfluidic system with two walls, placed at $x = 0$ and $x = L$ vibrating with the angular frequency ω. The amplitude of the vibration is denoted by ℓ and the domain consists of water with the density ρ_{w} and speed of sound c_{w}.

To evaluate the magnitude of the complex number the squared length, $|Z|^2$, is considered

$$|Z|^2 \simeq \sin^2(k_0 L) + (\gamma k_0 L)^2 \cos^2(k_0 L). \tag{4.11}$$

Eq. (4.11) is similar to the equation for an ellipse given by

$$1 = \frac{x^2}{a^2} + \frac{y^2}{b^2}, \tag{4.12}$$

with $(x, y) = (\cos(k_0 L), \sin(k_0 L))$ and $a = \frac{1}{\gamma k_0 L}$ denoting the minor axis and $b = 1$ the major axis. The squared length $|Z|^2$ thus has minima for $\sin(k_0 L) = 0$, i.e.,

$$k_0 = \frac{n\pi}{L} \qquad n = 1, 2, 3... \tag{4.13}$$

Studying the resonance case where k_0 is given by Eq. (4.13) we are now allowed to use the approximations[1] $e^{\pm k_0 \gamma x} \simeq 1 \pm k_0 \gamma x$, and $e^{\pm ikL} \simeq (-1)^n (1 \mp k_0 \gamma L)$ in Eq. (4.3) which is valid when $k_0 \gamma L \ll 1$. Combining this with Eq. (4.2b) the reformulated boundary condition reads

$$A(-1)^n(1 - n\pi\gamma) + B(-1)^n(1 + n\pi\gamma) = -\omega\ell. \tag{4.14}$$

The constants A and B now depend on n and are determined using Eqs. (4.2a) and (4.14)

$$A = \begin{cases} \left(\frac{1}{2} + \frac{1}{n\pi\gamma}\right)\omega\ell, & \text{for } n \text{ even}, \\ \frac{1}{2}\omega\ell, & \text{for } n \text{ odd}, \end{cases} \tag{4.15}$$

$$B = \begin{cases} \left(\frac{1}{2} - \frac{1}{n\pi\gamma}\right)\omega\ell \quad , & \text{for } n \text{ even}, \\ \frac{1}{2}\omega\ell \quad , & \text{for } n \text{ odd}. \end{cases} \tag{4.16}$$

For n odd the constants are in the order of magnitude 10^0 whereas the constants are in the order of magnitude 10^6 for n even. In the latter case resonance occurs and in the following we therefore choose to consider only n even. By insertion of the coefficients (4.15) and (4.16) for n even the velocity reads

$$v(x,t) = \omega\ell\left[\left(\tfrac{1}{2} + \tfrac{1}{k_0\gamma L}\right)e^{ikx} + \left(\tfrac{1}{2} - \tfrac{1}{k_0\gamma L}\right)e^{-ikx}\right]e^{-i\omega t}, \qquad 0 < x < L, \quad 0 < t. \tag{4.17}$$

Taking the real part of the equation we derive the velocity

$$v(x,t) = \omega\ell\big[\cos(k_0 x)\cos(\omega t) + \tfrac{2}{n\pi\gamma}\sin(k_0 x)\sin(\omega t)\big], \quad \text{for } n \text{ even}. \tag{4.18}$$

Note that $\cos(k_0 x)$ is in phase and $\sin(k_0 x)$ is $\frac{\pi}{2}$ out of phase with the motion of the wall. Inserting the value for $\gamma \simeq 10^{-6}$ returns a huge velocity due to resonance.

To verify the derived velocity field the boundary conditions, cf. Eq. (4.2), are controlled

[1] A Taylor expansion is allowed due to the small value of γ.

and are seen to be satisfied. Furthermore the velocity field is found to be a solution to the wave equation (4.1).
From the resulting velocity field the pressure and density fields can now be found using Eqs. (2.7a) and (2.7b). Integrating with respect to t

$$\begin{aligned}\rho_1 &= -\rho_0 \int \partial_x v(x,t) dt \\ &= -\rho_0 k_0 \ell \left\{ \left[\sin(k_0 x) - \tfrac{2}{L} \cos(k_0 x) \right] \sin(\omega t) - \tfrac{2}{n\pi\gamma} \cos(k_0 x) \cos(\omega t) \right\}. \end{aligned} \tag{4.19}$$

The pressure is determined by multiplying the density by the squared sound velocity in water

$$\begin{aligned}p(x,t) &= c_{\mathrm{w}}^2 \rho(x,t) \\ &= -c_{\mathrm{w}}^2 \rho_0 k_0 l \left\{ \left[\sin(k_0 x) - \tfrac{2}{L} \cos(k_0 x) \right] \sin(\omega t) - \tfrac{2}{n\pi\gamma} \cos(k_0 x) \cos(\omega t) \right\}. \end{aligned} \tag{4.20}$$

To evaluate the approximated amplitude of velocity, density and pressure fields a simplification is made. From Eq. (4.18), (4.19) and (4.20) it is observed that the dominating term is the term containing γ in the denominator and the other terms can then be neglected. Using values given in table 3.1 estimates of the maximum value of the velocity, density and pressure read

$$v_{1,\max} = \frac{2\omega\ell}{n\pi\gamma} \simeq 6.6 \times 10^1 \text{ m s}^{-1}, \tag{4.21}$$

$$\rho_{1,\max} = \frac{2\rho_0 k_0 \ell}{n\pi\gamma} \simeq 2.0 \times 10^2 \text{ kg m}^{-3}, \tag{4.22}$$

$$p_{1,\max} = c_{\mathrm{w}}^2 \rho_{1,\max} \simeq 4.03 \times 10^8 \text{ Pa}. \tag{4.23}$$

Choosing $n = 6$ corresponds to three waves within the domain of length L. This is due to the definition of the wave number $k = \frac{2\pi}{\lambda} = \frac{n\pi}{L}$ which give $n = 6$ for $L = 3\lambda$. The estimated velocity can now be compared to the sound velocity c_{w} in water

$$\frac{v_{\max}}{c_{\mathrm{w}}} = \frac{6.6 \times 10^1 \text{ m s}^{-1}}{1.42 \times 10^3 \text{ m s}^{-1}} = 5 \times 10^{-2}. \tag{4.24}$$

The perturbation velocity is 5% of the sound velocity which is acceptable and the use of the perturbation method is thereby verified.

Within a system consisting of two vibrating walls the cases of resonance have been investigated with and without damping. Excluding damping we find resonance of infinite amplitude for n chosen as even. Including viscosity and thereby damping the amplitude is still of great order of magnitude causing a first order velocity field of the size 6.6×10^1 ms^{-1}. These findings are in compliance with the calculations of other, [10]. However experimental results indicates a first order velocity field of the size 1 mms^{-1}, [10].

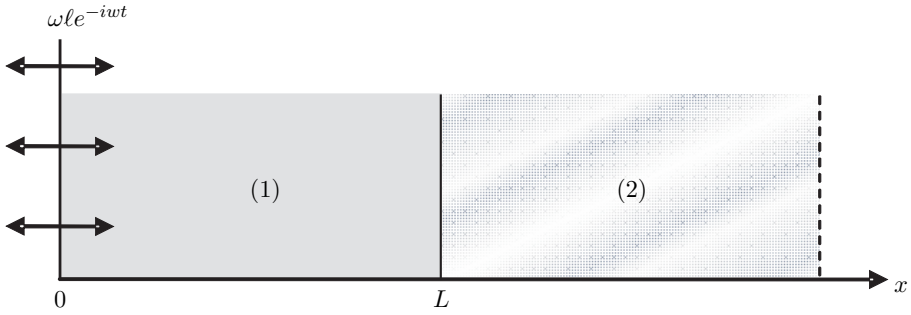

Figure 4.2: A sketch of the microfluidic system with one vibrating wall placed at $x = 0$ and a transition placed at $x = L$. The amplitude of the vibrating wall is denoted by ℓ.

Further the size of the piezo-induced pressure field in case of resonance, cf. Eq. (4.23,) is three orders of magnitude larger than the normal atmospheric pressure being 0.1 MPa. These findings suggest incorrectness of our calculations.

The perturbation theory is validated above, see Eq. (4.24), thus the sources of error must be found within our assumptions. The error may ensue from the given values of the system. Since the choice of ℓ is based on the measured amplitude of a piezo-actuator without loading, the choice $\ell = 10^{-10}$ m may be to large. Setting $v_{1,max} = 1$ mms^{-1} in Eq. (4.21) we find $\ell \simeq 10^{-15}$ m $n = 6$. Another explanation is energy accumulation in the system. This subject is discussed in the end of next section in relation to caparison of the findings of the present system and an two domain system.

4.2 Two domains enclosed by a piezo actuator and an absorbing wall

Now a system consisting of two domains are regarded. The right domain is assumed to be very thick compared to the domain of water and the outer boundary can thus be interpreted as an absorbing wall at rest, see Fig. 4.2. Choosing domain (1) as water and domain (2) as silicon we denote $c_1 = c_{\mathrm{w}}$, $c_2 = c_{\mathrm{Si}}$ and the zeroth order densities by $\rho_1 = \rho_{\mathrm{w}}$ and $\rho_2 = \rho_{\mathrm{Si}}$, see table 3.1.
Including attenuation the solution to the wave equation for v_1 Eq. (2.29) in one dimension for $0 < t$ reads

$$v_1(x,t) = (A_1 e^{ik_1 x} + B_1 e^{-ik_1 x})e^{-i\omega t}, \qquad 0 < x < L \tag{4.25}$$
$$v_2(x,t) = (A_2 e^{ik_2 x} + B_2 e^{-ik_2 x})e^{-i\omega t}, \qquad L < x < \infty \tag{4.26}$$
$$\tag{4.27}$$

where $k_1 = k_{01}(1 + i\gamma)$ and $k_{01} = \frac{\omega}{c_1}$, $k_2 = k_{02}(1 + i\gamma)$ and $k_{02} = \frac{\omega}{c_2}$. As in the in section 4.1 the wall placed at $x = 0$, see Fig. 4.2, vibrates with the velocity field

$$v(0,t) = \omega\ell e^{-i\omega t}, \tag{4.28}$$

which we saw leads to the boundary condition

$$\omega \ell = A_1 + B_1. \tag{4.29}$$

Looking at the wall between water and silicon, the velocity field and the pressure field must be continuous at the interior boundary condition. This implies the second and third boundary conditions

$$v_1(L) = v_2(L), \tag{4.30}$$
$$p_1(L) = p_2(L). \tag{4.31}$$

A final boundary condition we get from the assumption of the for $x \to \infty$. No reflecting waves are allowed in domain (2) and as a result the fourth boundary condition implies

$$B_2 = 0. \tag{4.32}$$

Using the four boundary conditions, Eqs. (4.29), (4.30), (4.31) and (4.32), expressions for the amplitudes are derived

$$A_1 = \frac{\omega l e^{-iLk_1}(c_2\rho_2 + c_1\rho_1)}{e^{iLk_1}(c_1\rho_1 - c_2\rho_2) + e^{-iLk_1}(c_1\rho_1 + c_2\rho 2)}, \tag{4.33a}$$

$$B_1 = \frac{\omega l e^{iLk_1}(c_1\rho_1 - c_2\rho_2)}{e^{iLk_1}(c_1\rho_1 - c_2\rho_2) + e^{-iLk_1}(c_2\rho_2 + c_1\rho_1)}, \tag{4.33b}$$

$$A_2 = \frac{2\omega l e^{-iLk_2} c_1\rho_1}{e^{iLk_1}(c_1\rho_1 - c_2\rho_2) + e^{-iLk_1}(c_1\rho_1 + c_2\rho 2)}. \tag{4.33c}$$

It is noted that if the matter in the two domains is identical, i.e., $c_1\rho_1 = c_2\rho_2$, $B_1 = 0$ and there will be no reflected wave. Further all the amplitudes are found to have the same denominator.

To determine which wave numbers lead to resonance the denominator of the coefficients are considered. The characteristic impedance is given by $Z_j = c_j\rho_j$ and using the relation $z_{12} = \frac{c_2\rho_2}{c_1\rho_1}$ and multiplying with e^{-ik_1L} in both numerator and denominator, the denominator in the three coefficients (4.33) reads

$$\begin{aligned} d &= (c_1\rho_1 - c_2\rho_2) + (c_1\rho_1 + c_2\rho_2)e^{-2ik_1L} \\ &= (1 - z_{12}) + (1 + z_{12})\big[\cos(2k_1L) - i(1 + z_{12})\sin(2k_1L)\big]. \end{aligned} \tag{4.34}$$

Using Taylor expansion of first order as done in previous section, Eq. (4.10), the denominator reads

$$\begin{aligned} d = (1 - z_{12}) &+ (1 + z_{12})\big[\cos(2k_{01}L) - i2\gamma k_{01}L\sin(2k_{01}L)\big] \\ &+ i(1 + z_{12})\big[\sin(2k_{01}L) + i2\gamma k_{01}L\cos(2k_{01}L)\big]. \end{aligned} \tag{4.35}$$

We define the squared length of the denominator as a function $f(k_01)$ of k_{01}. The function and its derivative read

$$f(k_1) = \Big\{(1-z_{12}) + (1+z_{12})\big[\cos(2k_1L) - 2\gamma k_{01}L\cos(2k_{01}L)\big]\Big\}^2 + \Big\{(1+z_{12})\big[\sin(2k_1L) - 2\gamma k_{01}L\sin(2k_{01}L)\big]\Big\}^2, \tag{4.36}$$

$$f'(k_1) = 4L(1+z_{12})\big[(z_{12}-1)\sin(2k_{01}L) + \gamma(...) + \gamma^2(...)\big]. \tag{4.37}$$

From Eq. (4.37) we find the function $f(k_{01})$ to approximately extremum at $k_{01} = \frac{n\pi}{2L}$ neglecting terms multiplied by γ and γ^2. To determine whether this value is a maximum or minimum the function $f(k_{01})$ is plotted in Fig. 4.3 with $z_{21} = \frac{c_2\rho_2}{c_1\rho_1}$. From the figure is found the first maximum value around $k_{01} \simeq 1600$ and the first minimum for $k_{01} \simeq 0$. Hence choosing n odd entails maximum whereas n even leads to minimum and thereby resonance. Thus we choose

$$k_{01} = \frac{n\pi}{2L}, \quad n \text{ even}. \tag{4.38}$$

In the zoom displayed right in Fig. 4.3 the minimum value of the squared length of denominator is seen to be approximately 4. This can also be found by insertion of Eq. (4.38) into Eq. (4.35) which gives $\frac{1}{2}$. Thus the denominator of the coefficients (4.33) equals 2 and we do not have a resonance of infinite amplitude.

Having determined k_{01} leading to resonance we find the corresponding value of k_{02}

$$k_{02} = k_{01}\frac{c_1}{c_2}, \quad n \text{ even}. \tag{4.39}$$

The value of k_{02} do not lead to resonance which is in accordance with domain (2) being enclosed by an absorbing wall in the one end. The following approximations apply: $e^{\pm ik_1L} \simeq$

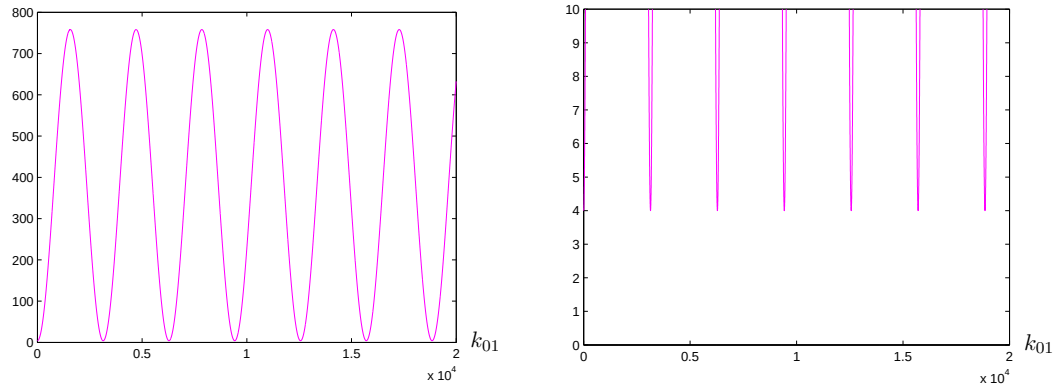

Figure 4.3: Plot of the squared length of the denominator $f(k_{01})$ as function of k_{01} for $z_{21} = \frac{c_2\rho_2}{c_1\rho_1}$. The zoom in the right figure reveals no intersections between the abscissa and the $f(k_{01})$.

$(-1)^{\frac{n}{2}}(1 \mp k_{01}\gamma L)$ and $e^{\pm k_{01}\gamma x} = 1 \pm k_{01}\gamma x$, together with $e^{\pm ik_2 L} \simeq (1 \mp k_{02}\gamma L)e^{\pm ik_{02}L}$ for n even. The expressions for the coefficients (4.33) can thus be reduced to

$$A_1 = \frac{\omega\ell(1 + k_{01}\gamma L)(c_1\rho_1 + c_2\rho 2)}{2(c_1\rho_1 + k_{01}\gamma L c_2\rho_2)}, \tag{4.40}$$

$$B_1 = \frac{\omega\ell(1 - k_{01}\gamma L)(c_1\rho_1 - c_2\rho_2)}{2(c_1\rho_1 + k_{01}\gamma L c_2\rho_2)}, \tag{4.41}$$

$$\mathrm{Re}(A_2) = \frac{2\omega\ell(1 + k_{02}\gamma L)c_1\rho_1 \cos(k_{02}L)}{(-1)^{\frac{n}{2}}(c_1\rho_1 + k_{01}\gamma L c_2\rho_2)}. \tag{4.42}$$

The latter constant, A_2, is in fact complex due to the approximation used for $e^{\pm ik_2 L}$. However in order to estimate the size the real part is displayed. By estimating the amplitudes we find $A_1 \simeq 2 \times 10^{-2}$, $B_1 \simeq -1.7 \times 10^{-2}$ and $A_2 \simeq -2.7 \times 10^{-3}$.

The velocity field is given by Eq. (4.25) and (4.26) in the respective domains setting $B_2 = 0$. Fig. 4.4 shows a plot of the velocity field in both domains. From the figure the wavelength of the velocity field in domain (2) is seen to be larger than the wavelength in domain (1). This is due to the physical parameters of the system entailing $k_{02} < k_{01}$ in response to $c_1 < c_2$. From the velocity field the density and pressure fields are determined in domain (1). ρ_0 thus denotes the constant zeroth order density term for water. Using Eqs. (2.7a) and (2.7b) in the following we have

$$\rho_1 = -\rho_0 \int \partial_x v_1(x,t)dt, \tag{4.43}$$

$$= -\rho_0(iA_1k_1e^{ik_1x} - iB_1k_1e^{-ik_1x})\tfrac{i}{\omega}e^{-i\omega t}. \tag{4.44}$$

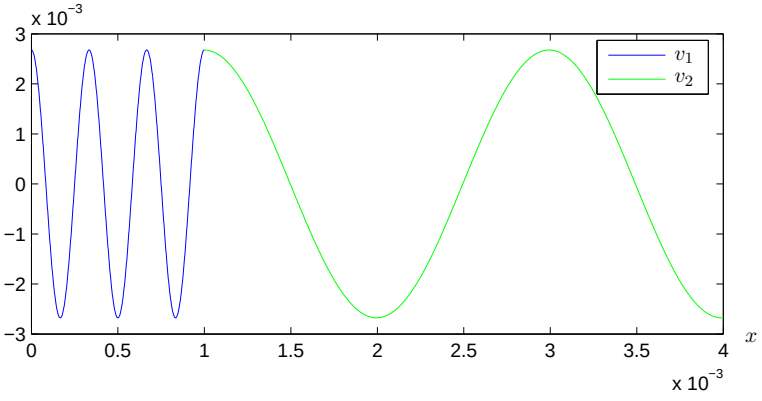

Figure 4.4: Plot of the velocity field for $n = 12$ in the two domain system with one vibrating wall placed at $x = 0$ and a transition placed at $x = L$. v_1 denotes the velocity field in domain (1) containing water, whereas v_2 denotes the velocity field in domain (2) consisting of silicon.

Looking at the real part of (4.44) we find the density field within domain (1)

$$\rho_1 = \frac{\rho_0 k_1 \sin(k_1 x)}{\omega}(A_1 + B_1). \tag{4.45}$$

The corresponding pressure field is determined to

$$p_1 = \frac{c_1^2 \rho_0 k_1 \sin(k_1 x)}{\omega}(A_1 + B_1). \tag{4.46}$$

To evaluate the size of the acoustic fields in domain (1) the following estimates are found

$$v_1 = A_1 + B_1 \simeq 10^{-2} \text{ m s}^{-1}, \tag{4.47}$$

$$\rho_1 = \frac{\rho_0}{c_1}(A_1 + B_1) \simeq 10^{-2} \text{ kg m}^{-3}, \tag{4.48}$$

$$p_1 = c_1 \rho_0 (A_1 + B_1) \simeq 10^4 \text{ Pa}. \tag{4.49}$$

We have now studied the case of two domains enclosed by a vibrating wall and an absorbing wall. The model is set up to represent the reaction chamber containing water, domain (1), and the adjacent layer consisting of silicon, domain (2). Focusing on the acoustic fields within the reaction chamber the wave number causing resonance in first domain have been derived including attenuation. The acoustic fields in domain (2) thus rely on the resulting fields of domain (1).

We find the wave number causing resonance in domain (1) to be half size of the wave number derived for the one domain system in previous section. However demanding the same number of waves within the same length L in both of the systems we must choose the double value of n in the this system in relation to the system considered in previous section. Thus demanding the same number of waves we have the same wave numbers for both systems.

Determining the amplitudes of the acoustic fields, we deduce that if the media in domain (1) and domain (2) have the same characteristic impedance no wave will be reflected at the interior boundary. Further the estimated sizes of the acoustic fields within the first domain are approximately a factor 10^6 smaller than the corresponding sizes of fields estimated in previous section.

The findings can be explained by considering the physical impact of having different boundary conditions in the two systems. In the one domain system we have energy contributions from the two walls enclosing the system and the only energy loss results from inner friction due to viscosity. Excluding heat transfer to the surroundings the energy accumulates in the one domain system. Considering the first domain of the present system we have only one vibrating wall providing energy to the system. The waves escaping domain (1) are being transmitted into domain (2) where they extinguish when reaching the absorbing wall. In the present system we therefore have loss of energy to the surroundings resulting in smaller amplitudes of the acoustic fields than those found in the one domain system.

With an absorbing wall we have energy outflow from the system. By adding a further layer to the system not all waves of the acoustic fields leave the system. Some are to be reflected which enables resonance within the first domain. Even though a perfect absorbing wall is not feasible in reality we find that extending the one domain system by adding a further domain and enabling energy outflow lead to acoustic fields of sizes more in accordance with experimental findings by others.

Chapter 5

Circular micro systems

An other proposed geometrical design of micro system useful for lab-on-a-chip devices is the circular design. In this chapter this type of system is investigated with examples of one and two domains using various boundary conditions. General solutions to the given systems are derived and the main difference from the previous one dimensional models is that now the solutions is a linear combination of the Bessel functions instead of the trigonometric functions. Furthermore the circular model is more realistic being two dimensional, however we have chosen the symmetric case. The emphasis of all the considered systems lies on determination of conditions for resonance.

First a system of one domain consisting of water with an encircling piezo actuator is regarded. Next a two domain system consisting of water and silicon with the encircling piezo actuator placed at the boundary of the outer domain is regarded. In the final considered system the piezo actuator is placed at the interior boundary.

As in previous chapter each of the models is sketched in a figure. However due to the study of different boundary conditions within some of the systems, inscription of specific boundary conditions are not included in the figures.

5.1 One domain with an encircling piezo actuator

We now consider a circular problem given in polar coordinates. The geometry of the system is a circular channel of radius $r = a$, see Fig. 5.1. We wish to determine the first order velocity, pressure and density field inside the circle assuming the time-dependency to be harmonic, $e^{-i\omega t}$. That is to solve the Helmholtz equation, Eq. (2.28),

$$\nabla^2\phi_1 = -k^2\phi_1, \tag{5.1}$$

where the Laplacian is given in polar coordinates $\nabla^2 = \partial_r^2 + \frac{1}{r}\partial_r + \frac{1}{r^2}\partial_\theta^2$. Damping is included, i.e., $k = k_0(1 + i\gamma)$ and ϕ_1 denotes the velocity potential given by

$$\phi_1 = \phi_1(r, \theta), \qquad 0 < r < a \ \text{ and } \ 0 < \theta < 2\pi. \tag{5.2}$$

The time-dependent velocity potential is found by multiplying the velocity potential with the harmonic factor $e^{-i\omega t}$, i.e., $\phi(r,\theta,t) = \phi(r,\theta)e^{-\omega t}$. Recalling Eqs. (2.14) and (2.7c) the velocity potential relates to the velocity field and the pressure field by

$$\mathbf{v}_1 = \boldsymbol{\nabla}\phi_1, \tag{5.3}$$
$$p_1 = -\rho_0\partial_t\phi_1. \tag{5.4}$$

The density field can be obtained using $\rho_1 = \frac{1}{c_0^2}p_1$, cf. Eq. (2.7a). Seeking time-dependent fields the time-dependent velocity potential must be applied. Having this in mind we are ready to determine the boundary conditions.

Due to causality, singularities at the center of the circular domain are not acceptable. The velocity potential must be bounded and the second bounded boundary condition therefore reads

$$|\phi_1(0,\theta)| < \infty. \tag{5.5a}$$

Regarding θ two other boundary conditions are needed. Demanding periodicity in θ for ϕ_1 and $\partial_\theta\phi_1$ the boundary conditions read

$$\phi_1(r,0) = \phi_1(r,2\pi), \tag{5.5b}$$
$$\partial_\theta\phi_1(r,0) = \partial_\theta\phi_1(r,2\pi). \tag{5.5c}$$

Expecting a product solution of the form $\phi_1 = R\Theta$, where $R = R(r)$ and $\Theta = \Theta(\theta)$, $R\Theta$ is inserted in the Helmholtz equation

$$\Theta R'' + \Theta\tfrac{1}{r}R' + \tfrac{1}{r^2}R\Theta'' = -k^2R\Theta, \tag{5.6}$$
$$r^2\frac{R''}{R} + r\frac{R'}{R} + r^2k^2 = -\frac{\Theta''}{\Theta}, \tag{5.7}$$

where $R' = \frac{d}{dr}R$, $R'' = \frac{d^2}{dr^2}R$ and $\Theta'' = \frac{d^2}{d\theta^2}\Theta$. Since the left-hand-side of Eq. (5.7) is independent of the right-hand-side both sides must equal the same constant μ^2. The two

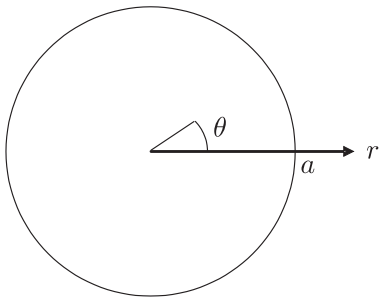

Figure 5.1: A sketch of the microfluidic system consisting of one domain consisting water encircled by a wall placed at $r = a$.

ordinary differential equations thus read

$$r^2\frac{R''}{R} + r\frac{R'}{R} + r^2k^2 = \mu^2, \tag{5.8}$$

$$\frac{\Theta''}{\Theta} = -\mu^2. \tag{5.9}$$

Seeking periodic solutions for Θ the sign of μ^2 is chosen to be positive. The ordinary differential equation for Θ, Eq. (5.9), has the known general solution

$$\Theta(\theta) = C_1 e^{-i\mu\theta} + C_2 e^{i\mu\theta}. \tag{5.10}$$

The boundary condition given by Eq. (5.5b) can be reformulated inserting the product solution $R(r)\Theta(0) = R(r)\Theta(2\pi)$ to $\Theta(0) = \Theta(2\pi)$, because $R(r) = 0$ only gives trivial solutions. Using the boundary condition leads to

$$C_1 + C_2 = C_1 e^{-i\mu 2\pi} + C_2 e^{i\mu 2\pi}. \tag{5.11}$$

For the equation to be fulfilled μ must be an integer m. Choosing $m \in \mathbb{Z}$ the solution reads

$$\Theta_m(\theta) = B_m e^{im\theta}, \qquad m \in \mathbb{Z}. \tag{5.12}$$

We see that this solution also fulfills the boundary condition given by Eq. (5.5c) as demanded. Returning to the ordinary differential equation for R, Eq. (5.8), the equation can be rewritten using $\mu^2 = m^2$

$$r^2R'' + rR' + (r^2k^2 - m^2)R = 0. \tag{5.13}$$

This is the parametric form of the Bessel equation of order m. The general solution to this equation is a linear combination of the Bessel functions of the first and second kind

$$R_m(r) = D_{1m}J_m(kr) + D_{2m}Y_m(kr). \tag{5.14}$$

The first three Bessel functions of first and second kind are given in Figs. 5.2 and 5.3 and the roots of the Bessel function of the first kind are given in table (5.1).

As for Θ the boundary condition given by Eq. (5.5a) must be reformulated to only concern

	$m=0$	$m=1$	$m=2$	$m=3$
	2.4048	3.8317	5.1356	6.3802
$J_m(x)$	5.5201	7.0156	8.4172	9.7610
	8.6537	10.1735	11.6198	13.0152
	11.7915	13.3237	14.7960	16.2235

Table 5.1: Values for approximate zeros of the Bessel function of the first kind. As $n \to \infty$ the roots differ approximately by π.

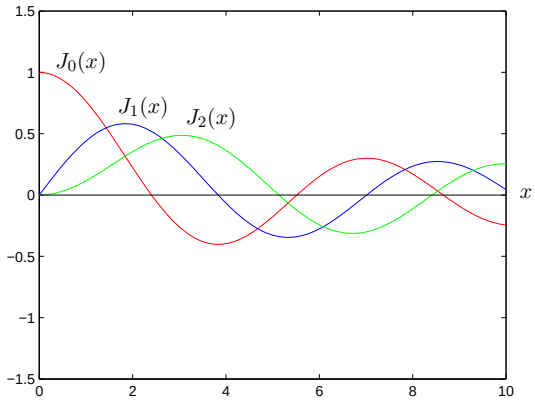

Figure 5.2: The first three Bessel functions of the first kind. Note $J_0(0) = 1$ whereas for all other choices of m $J_m(0) = 0$.

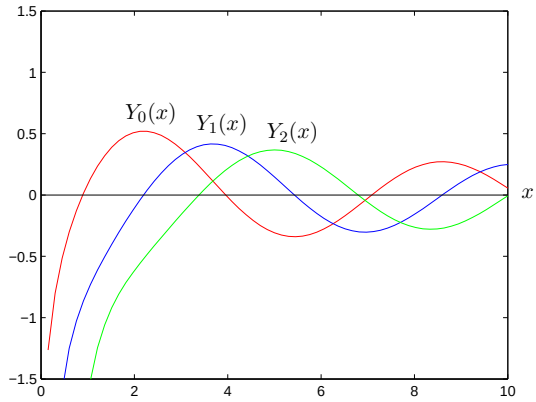

Figure 5.3: The first three Bessel functions of the second kind. Note for all functions $\lim_{x\to 0^+} Y_m(x) = -\infty$

$R(r)$. Inserting the product solution in the boundary condition $|R(0)\Theta(\theta)| < \infty$ gives the condition $|R(0)| < \infty$ due to causality. This implies D_2 in Eq. (5.14) must equal zero because $|Y_m(kr)|$ goes to infinity for r approaching 0^+, see Fig. (5.3). The solution thereby reads

$$R_{mn} = D_{1mn} J_m(k_{nm} r), \qquad m \in \mathbb{Z}, \quad n \in \mathbb{N}. \tag{5.15}$$

For a specific system k_{nm} is to be determined by a boundary condition. The index n is added because often n different values of k for each m satisfy a specific boundary condition.

The full solution to the time-independent Helmholtz equation in the given system is found by inserting the product solution $\phi_{mn}(r,\theta) = R_{mn}(r)\Theta_m(\theta)$ and multiplying the constants

$$\phi_1(r,\theta) = \sum_{m\in\mathbb{Z}} \sum_{m\in\mathbb{N}} A_{mn} J_m(k_n r)\, e^{im\theta}, \qquad 0 < r < a \quad \text{and} \quad 0 < \theta < 2\pi. \tag{5.16}$$

Including the time-dependency the velocity potential reads

$$\phi_1(r,\theta,t) = \sum_{m\in\mathbb{Z}} \sum_{n\in\mathbb{N}} A_{mn} J_m(k_n r)\, e^{im\theta} e^{-i\omega t}, \quad 0 < r < a, \quad 0 < \theta < 2\pi \quad \text{and} \quad 0 < t. \tag{5.17}$$

Using Eqs. (5.3), (5.4) and (2.7a) the general first order velocity, pressure and density fields are determined to

$$\mathbf{v}_1(r,\theta,t) = \sum_{m\in\mathbb{Z}} \sum_{n\in\mathbb{N}} A_{mn} \boldsymbol{\nabla} J_m(k_{mn} r)\, e^{im\theta} e^{-i\omega t}, \tag{5.18}$$

$$p_1(r,\theta,t) = -i\omega\rho_0 \sum_{m\in\mathbb{Z}} \sum_{n\in\mathbb{N}} A_{mn} J_m(k_{mn} r)\, e^{im\theta} e^{-i\omega t}, \tag{5.19}$$

$$\rho_1(r,\theta,t) = -\frac{i\omega\rho_0}{c_0^2} \sum_{m\in\mathbb{Z}} \sum_{n\in\mathbb{N}} A_{mn} J_m(k_{mn} r)\, e^{im\theta} e^{-i\omega t}, \tag{5.20}$$

for $0 < r < a$, $0 < \theta < 2\pi$ and $0 < t$. Note for polar coordinates $\boldsymbol{\nabla} = (\partial_r, \frac{1}{r}\partial_\theta)$.

5.1.1 The symmetric case in one domain

Choosing the symmetric case, i.e., $m = 0$, the solution becomes independent for θ and we use $\partial_r \mathbf{e}_r$ instead of $\boldsymbol{\nabla}$. The full solution to the time-independent Helmholtz equation in the symmetric case reads

$$\phi_1(r,\theta) = \sum_{n\in\mathbb{N}} A_n J_0(k_n r), \qquad 0 < r < a \ \text{ and } \ 0 < \theta < 2\pi. \tag{5.21}$$

Including the time-dependency the velocity potential reads

$$\phi_1(r,\theta,t) = \sum_{n\in\mathbb{N}} A_n J_0(k_n r) e^{-i\omega t}, \quad 0 < r < a, \ \ 0 < \theta < 2\pi \ \text{ and } \ 0 < t. \tag{5.22}$$

Using

$$J_0'(x) = -J_1(x), \tag{5.23}$$

the first order velocity field given by $\mathbf{v}_1 = v_1 \mathbf{e}_r$ together with the pressure and density fields are determined to

$$\begin{aligned} v_1(r,\theta,t) &= -\sum_{n\in\mathbb{N}} A_n k_n J_1(k_n r) e^{-i\omega t}, & (5.24)\\ p_1(r,\theta,t) &= i\omega\rho_0 \sum_{n\in\mathbb{N}} A_n J_m(k_n r) e^{-i\omega t}, & (5.25)\\ \rho_1(r,\theta,t) &= \frac{i\omega\rho_0}{c_0^2} \sum_{n\in\mathbb{N}} A_n J_0(k_n r) e^{-i\omega t}, & (5.26) \end{aligned}$$

for $0 < r < a, \ 0 < \theta < 2\pi$ and $0 < t$. The relation between the velocity field and the velocity potential read

$$\begin{aligned} \mathbf{v}_1 &= \partial_r \phi_1 \mathbf{e}_r, & (5.27)\\ v_1 &= \partial_r \phi_1, & (5.28) \end{aligned}$$

and we are thus allowed to perform the following calculations scalar.

5.1.2 One domain including attenuation

Having determined the symmetric solution to the Helmholtz equation in one circular domain we now seek specific solution with the boundary condition

$$\partial_r \phi(a,\theta) = \omega \ell \tag{5.29}$$

is applied. Physically the boundary condition can be interpreted as the encircling wall vibrating in time with the amplitude ωl symmetric in θ-coordinate. In the considered physical system only one angular frequency is present and therefore only one value for $k = k_n = k_{0n}(1 + i\gamma)$. This reduces the system to

$$\begin{aligned} \phi_n(r,\theta) &= A_n J_0(k_n r), & (5.30)\\ \partial_r \phi_n(r,\theta) &= -k_n A_n J_1(k_n r). & (5.31) \end{aligned}$$

The index m is excluded since it is set to zero. To determine $\partial_r \phi_n(r,\theta)$ we have used the identity given by Eq. (5.23). Seeking to determine the amplitude A_n a Taylor expansion around $k_0 r$ of the Bessel function $J_1(k_n r)$ reads

$$\begin{aligned} J_1(k_n r) &= J_1(k_{0n} r + i\gamma k_{0n} r), && (5.32)\\ &\simeq J_1(k_{0n} r) + J_1'(k_{0n} r)(i\gamma k_{0n} r) + \frac{J_1''(k_{0n} r)}{2}(i\gamma k_{0n} r)^2. && (5.33) \end{aligned}$$

Using the identities

$$\begin{aligned} x J_n'(x) &= x J_{n-1}(x) - n J_n(x), && (5.34a)\\ J_n'' &= \tfrac{1}{4}[J_{n-2}(x) - 2J_n + J_{n+2}(x)], && (5.34b)\\ J_{-n}(x) &= (-1)^n J_n(x), && (5.34c) \end{aligned}$$

gives

$$J_1(k_n r) \simeq J_1(k_{0n} r) + i\gamma\big[k_{0n} r J_0(k_{0n} r) - J_1(k_{0n} r)\big] - \frac{(\gamma k_{0n} r)^2}{8}\big[J_3(k_{0n} r) - 3J_1(k_{0n} r)\big]. \quad (5.35)$$

Inserting this result into Eq. (5.30) and using the boundary condition given by Eq. (5.29) entails

$$\begin{aligned} \omega \ell &= -k_n A_n J_1(k_n a), && (5.36)\\ A_n &\simeq -\frac{k_n^{-1}\omega\ell}{\big\{J_1(k_{0n}a) + i\gamma\big[k_{0n}aJ_0(k_{0n}a) - J_1(k_{0n}a)\big] - \frac{(\gamma k_{0n}a)^2}{8}\big[J_3(k_{0n}a) - 3J_1(k_{0n}a)\big]\big\}}. && (5.37) \end{aligned}$$

The amplitude A_n is dependent on the choice of k_{0n}. To examine at which value of k_{0n} resonance is present in the system, the squared length of the complex denominator Z of A_n given by Eq. (5.37) is considered.

$$\begin{aligned} |Z|^2 &= \Big(J_1(k_{0n}a) - \tfrac{(\gamma k_{0n}a)^2}{8}\big[J_3(k_{0n}a) - 3J_1(k_{0n}a)\big]\Big)^2 + \Big(\gamma\big[k_{0n}aJ_0(k_{0n}a) - J_1(k_{0n}a)\big]\Big)^2, && (5.38)\\ &= J_1^2(k_{0n}a) + \gamma^2(...) + \gamma^4(...). && (5.39) \end{aligned}$$

The squared length is separated in three terms with the prefactors 1, γ^2 and γ^4. The size of $k_{0n}a$ is in the order of magnitude 10^0, when considering a circular domain with radius $a = 1$ mm containing water. The difference in order of magnitude between the three terms is therefore almost exclusively determined by the prefactors. Due to the small size of γ the two last terms can be neglected. Resonance is thereby found for $J_1(k_{0n}a) = 0$ which is to say

$$k_{1n} = \frac{\alpha_{1n}}{a}, \quad (5.40)$$

where α_{1n} is the n'th root of J_1. The definition of the wave number $k_0 = \frac{2\pi}{\lambda}$ gives us together with table 5.1 the wavelengths corresponding to the three first roots of J_1.

$$\lambda_1 = 1.64 \times 10^{-3} \text{ m}, \qquad \lambda_2 = 8.96 \times 10^{-4} \text{ m}, \qquad \lambda_3 = 6.18 \times 10^{-4} \text{ m}. \tag{5.41}$$

It must be remarked that the "wavelength" of a wave given by the Bessel functions is not a constant. However the "wavelength" gives a good estimate of which number of root to choose. By selecting the third root and thereby the third of the wavelengths we have approximately three waves within the diameter of the system, $2a = 2$ mm. With $n = 3$ the wave number, cf. Eq. (5.40), and thereby also the angular frequency is given by

$$k_0 = 1.02 \times 10^4 \text{ m}^{-1}, \qquad \omega = 1.44 \times 10^7 \text{ s}^{-1}. \tag{5.42}$$

The full solution of the system with the specific boundary condition given by Eq. (5.29) reads

$$\phi(r, \theta) \quad = \quad A_{03} J_0(k_3 r), \qquad k_3 = \frac{\alpha_{03}}{a}(1 + i\gamma), \tag{5.43}$$

where A_{03} is given by Eq. (5.37) for $n = 3$. In Fig. 5.4 the solution with no attenuation, i.e., $k_n = k_{0n}$, is shown for $n = 1, 2, 3$. Parameters for water are used and the radius of the system is set to $a = 1$ mm. As stated above $n = 1$ is seen to give rise to one wave, $n = 2$ to two waves and $n = 3$ to three waves within the chamber of diameter $2a$, respectively. The slopes of the different functions near the boundary $r = a$ are due to the boundary condition Eq. (5.29) expected to be constant. However in Fig. 5.4 the slopes appear to

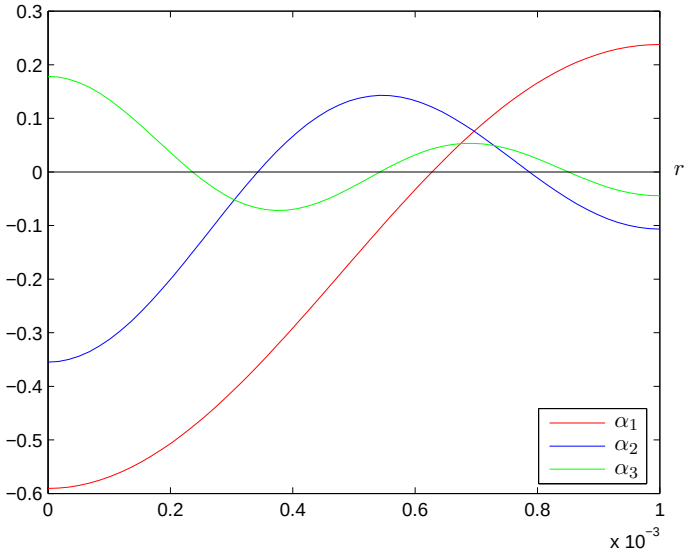

Figure 5.4: Plot of $\phi(r) = A_n J_0(k_{0n} r)$ for $n = 1, 2, 3$, where $A_n = -\frac{\omega_n \ell}{k_{0n} J_1(k_{0n} a)}$, $k_{0n} = \frac{\alpha_{1n}}{a}$ and α_{1n} are the n'th root of J_1.

be zero. They are in fact zero because the solution is plotted with no attenuation and therefore the derivative, $J_1(k_3 r)$, is zero at $r = a$, cf. Eq. (5.40).

Including the time-dependency the solution reads

$$\phi(r,\theta,t) = A_3 J_0(k_3 r)\, e^{-i\omega t}, \quad 0 < r < a, \;\; 0 < \theta < 2\pi \;\text{ and }\; 0 < t. \tag{5.44}$$

Using Eqs. (5.3), (5.4) and (2.7a) together with the identities Eq. (5.34a) the first order velocity, pressure and density fields are determined to be

$$\mathbf{v}_1(r,\theta,t) = -k_3 A_3 J_1(k_3 r) e^{-i\omega t}\mathbf{e}_r, \tag{5.45}$$

$$p_1(r,\theta,t) = i\omega\rho_0 A_3 J_0(k_3 r) e^{-i\omega t}, \tag{5.46}$$

$$\rho_1(r,\theta,t) = \frac{i\omega\rho_0}{c_1^2} A_3 J_0(k_3 r) e^{-i\omega t}, \tag{5.47}$$

for $0 < r < a$, $0 < \theta < 2\pi$ and $0 < t$. Taking the real parts of the fields and determining their maximum values yield

$$v_1 = \omega\ell \frac{x}{x^2 + y^2} \simeq 1.64 \times 10^2 \text{ m s}^{-1}, \tag{5.48}$$

$$p_1 = \frac{\rho_0 \omega^2 \ell}{k_{03}} \frac{\gamma x + y}{(\gamma+1)(x^2+y^2)} \simeq 7.4 \times 10^7 \text{ Pa}, \tag{5.49}$$

$$\rho_1 = \frac{p_{1\max}}{c_1^2} \simeq 3.67 \times 10^1 \text{ kg m}^{-3}, \tag{5.50}$$

where

$$x = J_1(k_{03}a) - \tfrac{(\gamma k_{03} a)^2}{8}\big[J_3(k_{03}a) - 3J_1(k_{o3}a)\big], \tag{5.51}$$

$$y = \gamma\big[k_{03} a J_0(k_{03}a) - J_1(k_{03}a)\big]. \tag{5.52}$$

The general solution to the Helmholtz equation in polar coordinates have been derived in order to study the a circular domain enclosed by a piezo wall. The symmetric case is studied reducing the number of dependent coordinates to one. Thus the system is independent of θ. The acoustic fields have been derived with respect to the wave numbers causing cases of resonance.

For reference we compare our findings with the ones of the one domain system enclosed by two vibrating walls, see section 4.1. This is done because the boundary conditions of the two given systems are similar by the means of the piezo actuator inducing vibrations of the entire boundary leaving no possibility of energy outflow.

Estimating the amplitudes of the acoustic fields we find a larger velocity field for the present system than for the one dimensional system. Concerning pressure and therefore also density we in contrast find smaller fields in the present system than in the first system.

The findings suggest that an encircling piezo actuator induces a larger velocity field. Due to the geometry of the circular the liquid within the system are affected radially.

In the ending of section 4.2 a comparison of the acoustic fields derived for the one dimensional systems were done. Here it was found that the acoustic fields were overall decreased by the same order of magnitude when expanding the one domain system to two domains. However attempting to compare the acoustic fields of present system and the one dimensional consisting of one domain, we do not find the same relation.

5.2 Two concentric domains with an encircling piezo actuator

We now add an extra layer to the circular domain described in the previous section. The system now consist of one inner circular domain containing water and one outer circular domain of silicon, denoted domain (1) and domain (2), respectively. The radius of domain (1) is $r = a$ and the radius of domain (2) is $r = b$, see Fig. 5.5. The time-dependency is still assumed harmonic, $e^{-i\omega t}$. Seeking determination of the velocity, pressure and density field in the system, the Helmholtz equation for ϕ in first order perturbation, Eq. (2.28), is to be solved. Having two domains the indices of ϕ denotes the number of domain an not the order of perturbation. Given no index indicates the entire solution. The Helmholtz equation of the full problem reads

$$\nabla^2\phi = -k^2\phi, \tag{5.53}$$

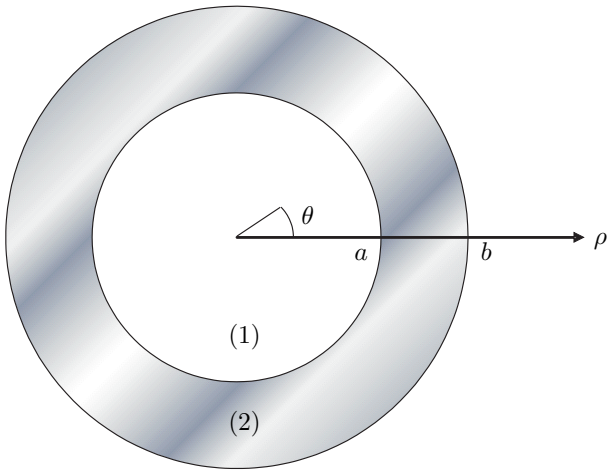

Figure 5.5: A sketch of the microfluidic system consisting of an inner circular domain of water and an outer domain of silicon. The inner domain, domain (1), is separated from the outer domain, domain (2), by a circular wall placed at $r = a$. The outer domain is encircled by a wall placed at $r = b$.

where attenuation is present, i.e., $k = k_0(1 + i\gamma)$, and ϕ denotes the velocity potential given by

$$\phi(r,\theta) = \begin{cases} \phi_1(r,\theta) & 0 < r < a \ \text{ and } \ 0 < \theta < 2\pi, \\ \phi_2(r,\theta) & a < r < b \ \text{ and } \ 0 < \theta < 2\pi. \end{cases} \tag{5.54}$$

The time-dependent velocity potential reads

$$\phi(r,\theta,t) = \phi(r,\theta)e^{-i\omega t}, \quad 0 < r < a, \ \ 0 < \theta < 2\pi \ \text{ and } \ 0 < t. \tag{5.55}$$

As in the system consisting of one circular domain we demand a finite velocity potential at the center and periodicity in θ. Thus the boundary conditions read

$$|\phi_1(0,\theta)| < \infty, \tag{5.56a}$$
$$\phi_{1,2}(r,0) = \phi_{1,2}(r,2\pi), \tag{5.56b}$$
$$\partial_\theta\phi_{1,2}(r,0) = \partial_\theta\phi_{1,2}(r,2\pi). \tag{5.56c}$$

Using same approach as in section 5.1 with the boundary conditions Eqs. (5.56a), (5.56b) and (5.56c) we get the general solution

$$\phi(r,\theta) = \begin{cases} \displaystyle\sum_{m\in\mathbb{Z}}\sum_{n\in\mathbb{N}} A_{mn}J_m(k_{1,mn}r)\, e^{im\theta} & 0 < r < a \ \text{ and } \ 0 < \theta < 2\pi, \\ \displaystyle\sum_{m\in\mathbb{Z}}\sum_{n\in\mathbb{N}} \left[B_{mn}J_m(k_{2,mn}r) + C_{mn}Y_m(k_2r)\right] e^{im\theta} & a < r < b \ \text{ and } \ 0 < \theta < 2\pi. \end{cases} \tag{5.56d}$$

It is noted that the second kind of the Bessel function Y_m exists in domain (2). Y_m has no singularities in this domain and can therefore not be excluded due to a bounded boundary condition. The velocity, pressure and density field can be obtained using Eqs. (5.3), (5.4) and (2.7a).

As in the case of one domain, section 5.1, $k_{1,mn}$ and $k_{2,mn}$ are not determined in the general solution. Further boundary conditions are required. Demanding continuity of the velocity and pressure field in the limit between the two domains gives the boundary conditions

$$\boldsymbol{\nabla}\phi_1(a,\theta) = \boldsymbol{\nabla}\phi_2(a,\theta), \tag{5.56e}$$
$$\rho_1\phi_1(a,\theta) = \rho_2\phi_2(a,\theta). \tag{5.56f}$$

Applying these boundary conditions together with a specific condition on the boundary, $r = b$, the wave numbers $k_{1,mn}$ and $k_{2,mn}$ can be determined.

5.2.1 The symmetric case in two domains

Analogues with section 5.1.1 the full solution to the time-independent Helmholtz equation in the symmetric case reads

$$\phi(r,\theta) = \begin{cases} \sum_{n\in\mathbb{N}} A_n J_0(k_{1,n} r) & 0 < r < a \text{ and } 0 < \theta < 2\pi, \\ \sum_{n\in\mathbb{N}} \left[B_n J_0(k_{2,n} r) + C_n Y_0(k_{2,n} r) \right] & a < r < b \text{ and } 0 < \theta < 2\pi. \end{cases} \tag{5.57}$$

The velocity, pressure and density field can be obtained using Eqs. (5.3), (5.4) and (2.7a) together with the relations Eqs. (5.28) and (5.28).

$k_{1,n}$ and $k_{2,n}$ are to be determined demanding continuity of the velocity and pressure field in the limit between the two domains

$$\partial_r \phi_1(a,\theta) = \partial_r \phi_2(a,\theta), \tag{5.58a}$$
$$\rho_1 \phi_1(a,\theta) = \rho_2 \phi_2(a,\theta), \tag{5.58b}$$

and applying a specific condition on the boundary $r = b$.

5.2.2 Natural oscillations

We now wish to consider the system of water in domain (1) and silicon in domain (2), see table 3.1 for parameter values. To the system we now add the specific boundary condition

$$\partial_r \phi(b,\theta) = 0, \tag{5.59}$$

and thus demanding zero normal velocity at the external boundary. The differential equation to solve is the Helmholtz equation. Excluding attenuation the solution to this system is either the zero solution where $A_n = B_n = C_n = 0$ with arbitrary wave numbers or free oscillations with arbitrary amplitudes and finite real wave numbers, $k_{1,n} = k_{01,n}$ and $k_{1,n} = k_{01,n}$.

We will now determine the wave numbers for the case with no attenuation and arbitrary constants. Applying the boundary condition Eq. (5.59) and using the identities given by Eq. (5.23) leads to

$$0 = -B_n k_{02,n} J_1(k_{02,n} b) - C_n k_{02,n} Y_1(k_{02,n} b), \tag{5.60}$$
$$0 = \frac{Y_1(k_{02,n} b)}{J_1(k_{02,n} b)} + \frac{B_n}{C_n}. \tag{5.61}$$

$k_{02,n}$ cannot be determined analytically, but must be determined numerically. To do this we must know approximately which values of $k_{02,n}$ to expect. We demand one to four waves within the inner circular chamber, domain (1), with the radius $a = 1$ mm. Recalling that domain (1) consists of water and domain (2) of silicon gives wavelengths and thus wave numbers within the intervals

$$5 \times 10^{-4} \text{ m} < \lambda_1 < 2 \times 10^{-3} \text{ m}, \tag{5.62}$$
$$3.15 \times 10^{3} \text{ m}^{-1} < k_{01,n} < 1.26 \times 10^{4} \text{ m}^{-1}. \tag{5.63}$$

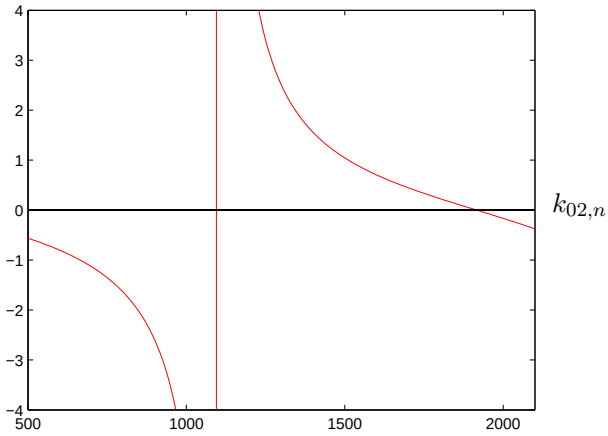

Figure 5.6: Graphical determination of $k_{02,n}$ for free oscillations in the symmetric case. The ratio $\frac{B}{C}$ is set to zero.

Since the angular frequency is constant within the system the relation

$$k_{01,n}c_1 = k_{02,n}c_2, \tag{5.64}$$

enable us to determine the interval for $k_{02,n}$

$$5.25 \times 10^2 \text{ m}^{-1} < \quad k_{02,n} \quad < 2.10 \times 10^3 \text{ m}^{-1}. \tag{5.65}$$

We are now ready to numerically determine a solution to Eq. (5.61). First the function

$$f(k_{02,n}) = \frac{Y_1(k_{02,n}b)}{J_1(k_{02,n}b)} + \frac{B_n}{C_n}. \tag{5.66}$$

is plotted in the interval given by Eq. (5.65) choosing $B = 0$. $k_{02,n}$ can therefore be determined as the intersections with the abscissa, see Fig. 5.6. From the figure is seen one intersection, which must be determined numerically. The intersection depends on the ratio $\frac{B}{C}$, which in the figure is set to zero. Setting the ratio to e.g. one corresponds to an elevation of the abscissa by one and thereby other intersections. Even though the amplitudes are arbitrary the solutions for $k_{01,n}$ and $k_{02,n}$ depend on the mutual relation between the constants in domain (2).

Having determined the wave number $k_{2,n}$ numerically in domain (2), $k_{1,n}$ can be found by using Eq. (5.64)

$$k_{01,n} = k_{02,n}\frac{c_2}{c_1}. \tag{5.67}$$

An equation and a method of approach have been suggested in order to determine the

wave numbers causing free oscillations in the unaffected system. The wave numbers in both domains are found to depend directly on the ratio of the coefficients in the second domain. This is a consequence of zero velocity at the outer boundary. Moreover the demand of continuity within the pressure and velocity fields at the interior boundary leads to the coefficients in both domains being determined by the physical parameters of the overall system.

5.2.3 Two domains including attenuation

We now wish to determine the amplitudes arising in the symmetric case with the specific boundary condition for $r = b$

$$\partial_r \phi_2(b, \theta) \quad = \quad \omega \ell \tag{5.68}$$

together with the two general boundary conditions demanding continuity in velocity and pressure at the interior boundary $r = a$, given by Eqs. (5.58a) and (5.58b). The three boundary conditions give together with the identity $J_0'(kx) = -kJ_1(x)$ the three equations

$$\omega \ell \quad = \quad -B_n k_{2,n} J_1(k_{2,n} b) - C_n k_{2,n} Y_1(k_{2,n} b), \tag{5.69}$$

$$A_n \rho_1 J_0(k_{1,n} a) \quad = \quad B_n \rho_2 J_0(k_{2,n} a) + C_n \rho_2 Y_0(k_{2,0} a), \tag{5.70}$$

$$-A_n k_{1,n} J_1(k_{1,n} a) \quad = \quad -B_n k_{2,n} J_1(k_{2,n} a) - C_n k_{2,n} Y_1(k_{2,0} a), \tag{5.71}$$

with the amplitudes A_n, B_n and C_n as the three unknowns. For simplicity we denote the coefficients to the amplitudes by letters as given in table 5.2. The three equations become

$$\omega \ell \quad = \quad -B_n x - C_n y, \tag{5.72}$$

$$A_n o \quad = \quad B_n p + C_n q, \tag{5.73}$$

$$-A_n r \quad = \quad -B_n s - C_n t, \tag{5.74}$$

	$x = k_{2,n} J_1(k_{2,n} b)$	$y = k_{2,n} Y_1(k_{2,n} b)$
$o = \rho_1 J_0(k_{1,n} a)$	$p = \rho_2 J_0(k_{2,n} a)$	$q = \rho_2 Y_0(k_{2,0} a)$
$r = k_{1,n} J_1(k_{1,n} a)$	$s = k_{2,n} J_1(k_{2,n} a)$	$t = k_{2,n} Y_1(k_{2,0} a)$

Table 5.2: Denoting coefficients with letters for simplification.

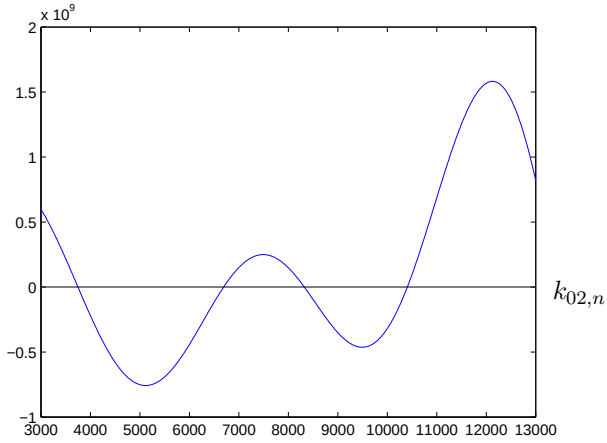

Figure 5.7: Graphical determination of the value of $k_{01,n}$ causing resonance .

having the solution

$$A_n = \frac{-\omega_n \ell(qs - pt)}{r(qx - py) + o(sy - tx)}, \tag{5.75}$$

$$B_n = \frac{-\omega_n \ell(qr - ot)}{r(qx - py) + o(sy - tx)}, \tag{5.76}$$

$$C_n = \frac{-\omega_n \ell(pr - os)}{r(qx - py) + o(sy - tx)}. \tag{5.77}$$

The three amplitudes are given by the same denominator and resonance therefore occurs at the same choice of $k_{1,n}$ and $k_{2,n}$ for all amplitudes. Setting the denominator equal to zero gives the equation

$$0 = r(qx - py) + o(sy - tx). \tag{5.78}$$

The relation between $k_{01,n}$ and $k_{02,n}$ given by Eq. (5.64) is valid whether or not attenuation is included. Thus $k_{2,n}$ can be expressed in terms of $k_{1,n}$ and substituted into Eq. (5.78). Thereby the equation has only one unknown, $k_{1,n}$, which using Taylor expansion can be determined numerically. The equation is plotted in Fig. 5.7 for $k_{01,n}$ on the interval given by Eq. (5.63) determined in previous section. The solutions for $k_{01,n}$ are to be found where the graph intersects with the abscissa. Numerically $k_{01,n}$ is determined choosing $n = 3$

$$k_{01,3} = 1.0406 \times 10^4 \text{ m}^{-1}, \tag{5.79}$$

corresponding to $\lambda = 6.03 \times 10^{-4}$ m, $k_{02,3} = 1.738 \times 10^3$ m^{-1} and $\omega_n = 1.477 \times 10^7$ s^{-1}. The index n will be left out in the further notation. Using Eqs. (5.76), (5.77) and (5.77)

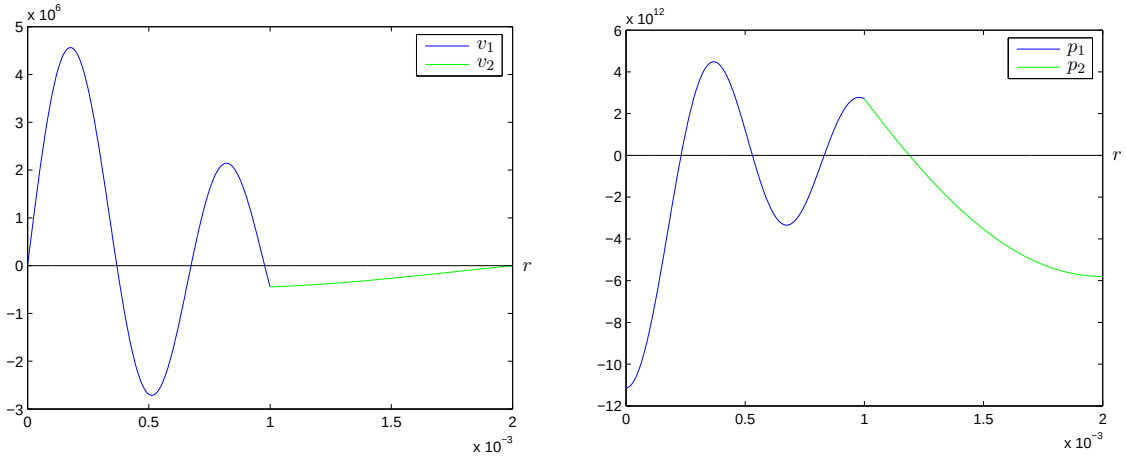

Figure 5.8: Left the velocity field and right the pressure field in the circular two domain system enclosed by an encircling piezo actuator for $0 < r < b$, $b = 2$ mm. The interior boundary is placed at $x = a$, $a = 1$ mm.

the constants are determined to

$$A_n = -753.46 \text{ m}^2\text{s}^{-1}, \tag{5.80}$$

$$B_n = 380.64 \text{ m}^2\text{s}^{-1}, \tag{5.81}$$

$$C_n = -137.11 \text{ m}^2\text{s}^{-1}. \tag{5.82}$$

By insertion of the constants in Eq. (5.57) the velocity potential is fully determined. From this the acoustic fields can be found using Eqs. (5.28) and (5.4). In Fig. 5.8 the velocity and pressure are displayed. The density field is left out being proportional to the pressure field in each domain alone. An estimation of maximum value of the real part of the acoustic fields for domain (1)

$$v_1 < 8 \times 10^6 \text{ m s}^{-1}, \tag{5.83}$$

$$p_1 < 1 \times 10^{13} \text{ Pa}, \tag{5.84}$$

$$\rho_1 < 6 \times 10^6 \text{ kg m}^{-3}, \tag{5.85}$$

together with the fields for domain (2)

$$v_2 < 9 \times 10^3 \text{ m s}^{-1}, \tag{5.86}$$

$$p_2 < 2 \times 10^{13} \text{ Pa}, \tag{5.87}$$

$$\rho_2 < 2 \times 10^5 \text{ kg m}^{-3}. \tag{5.88}$$

Remark that the estimates are upper limits but not the true maximum values of the magnitude of the resulting fields. By looking at Fig. 5.8 we for instance find $v_1 \approx 4.5 \times 10^6$ m s^{-1}.

Overall the sizes of the first order acoustic fields within both domains are enormous compared to previous findings and experimental results by others, [10]. Hence we must reconsider the physical assumptions within the model.

The piezo actuator is now loaded by a silicon domain in stead of a water domain, which was the case for the one domain circular system. The piezo actuator can not be assumed to activate the silicon domain in with the same impact as in the case of water. By reducing the amplitude of the piezo-induced vibrations, the order of magnitude of the acoustic fields in the present system will be likewise reduced as a consequence of being directly proportional to ℓ.

Moreover the smaller compressibility of silicon compared to water explains why the first order perturbation in density in domain (2) is smaller than the corresponding in domain (1).

5.3 Two concentric domains with interior piezo actuator

We now consider a system of the same geometry as in the previous example, i.e., two concentric circular domains. Domain (1) consists of water whereas domain (2) consists of silicon. In contrast to the previous example the outer wall is now assumed to be an absorbing wall preventing waves in the second domain being reflected at the boundary. The Helmholtz equation, cf. Eq. (2.28), is to be solved with attenuation, i.e., $k_{mn} = k_{0,mn}(1+i\gamma)$. We choose the solution to the problem in the second domain as a combination of the Hankel functions contrary to the example in section 5.2. This choice of solution will show to be useful with the given boundary condition in the second domain. The same approach as in section 5.2 is used to derive the general solution to the problem replacing the Bessel functions of the first and the second kind with the Hankel functions in the second domain. The wave function present in domain (1) and domain (2) is defined as ϕ_1 and ϕ_2, respectively.

Demanding periodicity in θ referring to Eqs. (5.56b) and (5.56c) the velocity potential for this system reads

$$\phi_{mn}(r,\theta) = \begin{cases} \left[A_{mn}J_m(k_{1,mn}r) + B_{mn}Y_m(k_{1,mn}r)\right] e^{im\theta}, & 0 < r < a \ \text{ and } \ 0 < \theta < 2\pi \\ \\ \left[C_{mn}H_m^1(k_{2,mn}r) + D_{mn}H_m^2(k_2 r)\right] e^{im\theta}, & a < r < b \ \text{ and } \ 0 < \theta < 2\pi. \end{cases} \tag{5.89}$$

Requiring the same boundary condition, Eq. (5.56a), as in the previous examples the second kind of the Bessel function must be eliminated from ϕ_1 in Eq. (5.89) since Y_m approaches minus infinity for $r \to 0^+$ and does not fulfill the condition $|\phi(r,\theta)| < \infty$. Therefore B_{mn} is set to zero. Another boundary condition stems from the absorbing wall encircling the second domain. It cannot be allowed to have a wave propagating towards

the center and as a consequence D_{mn} equals zero. Left are the two remaining functions

$$\phi(r,\theta) = \begin{cases} \sum_{m\in\mathbb{Z}} \sum_{n\in\mathbb{N}} A_{mn} J_m(k_{1,mn} r)\, e^{im\theta}, & 0 < r < a \ \text{ and } \ 0 < \theta < 2\pi, \\ \sum_{m\in\mathbb{Z}} \sum_{n\in\mathbb{N}} C_{mn} H_m^1(k_{2,mn} r)\, e^{im\theta}, & a < r < b \ \text{ and } \ 0 < \theta < 2\pi, \end{cases} \tag{5.90}$$

where the time-dependent velocity potential $\phi(r,\theta,t)$ reads $\phi(r,\theta)e^{-i\omega t}$.

5.3.1 The symmetric case in two domains

Having symmetry we now reduce the solution given by Eq. (5.90) to

$$\phi(r,\theta) = \begin{cases} \sum_{n\in\mathbb{N}} A_n J_0(k_{1,n} r), & 0 < r < a \ \text{ and } \ 0 < \theta < 2\pi, \\ \sum_{n\in\mathbb{N}} C_n H_0^1(k_{2,n} r), & a < r < b \ \text{ and } \ 0 < \theta < 2\pi. \end{cases} \tag{5.91}$$

Using the same approach as for the symmetric case in one domain, see section 5.1.1, the boundary condition of ϕ_1 in the symmetric case of two domains reads

$$\partial_r \phi_1(a) = \omega \ell, \tag{5.92}$$

assuming a harmonic actuation as the oscillating acoustic field at $r = a$. For domain (1) the setup is identical to the one circular domain with encircling piezo actuator described in section 5.1.2. Domain (1) is not affected from domain (2) due to the piezo placed at the interior boundary. Since the system is simplified not to make allowance for the loading of

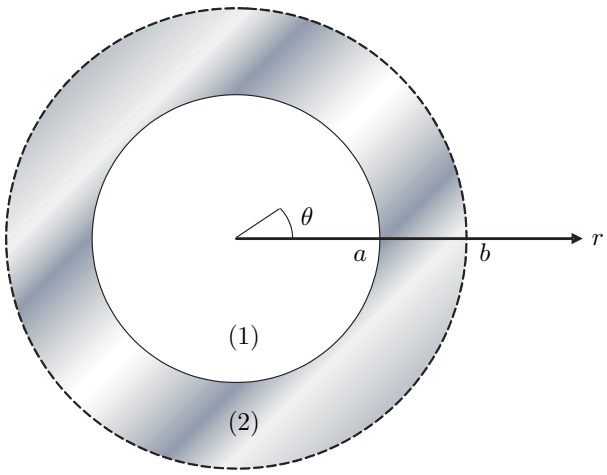

Figure 5.9: The microfluidic system consisting of two domains encircled by an absorbing wall placed at $r = b$. At $r = a$ a piezo actuator is placed which activates the acoustic waves. The external dashed circle represents the absorbing wall.

the piezo actuator. The resulting acoustic fields in domain (1) is therefore unaffected by the respective media in domain (2). Referring to section 5.1.2 the maximum values of the fields yields

$$v_1 \simeq 1.64 \times 10^2 \text{ m s}^{-1}, \tag{5.93}$$

$$p_1 \simeq 7.4 \times 10^7 \text{ Pa}, \tag{5.94}$$

$$\rho_1 \simeq 3.67 \times 10^1 \text{ kg m}^{-3}. \tag{5.95}$$

These are obtained by choosing $k_{01,3} = 1.02 \times 10^4 \text{ m}^{-1}$ thus $n = 3$ which is governed in the following derivations and thereby the index is discarded. Calculating the fields of domain (2) the following boundary condition is used

$$\partial_r \phi_2(a) = \omega \ell. \tag{5.96}$$

Inserting ϕ_2 and using $(H_0^1(x))' = -H_1^1(x)$ yields

$$C = \frac{-\omega \ell}{k_2 H_1^1 k_2 a}. \tag{5.97}$$

By making a Taylor expansion of H_1^1 the amplitude of domain (2) reads

$$C = \frac{-\omega \ell}{k_2 (H_1^1(k_{02}a) + \frac{i\gamma k_{02} a}{2}(H_0^1(k_{02}a) - H_2^1(k_{02}a)))}. \tag{5.98}$$

The fields for domain (2) can now be found using Eqs. (2.14) and (2.7c) with $\phi_2(r) = CH_0^1(k_2 r)$.

$$v_2 \simeq 2.02 \times 10^{-3} \text{ m s}^{-1}, \tag{5.99}$$

$$p_2 \simeq 8.39 \times 10^3 \text{ Pa}, \tag{5.100}$$

$$\rho_2 \simeq 1.1 \times 10^{-4} \text{ Pa s}. \tag{5.101}$$

The estimates just presented are here seen to be very small compared to the fields found in domain (1). This is caused by the given boundary condition having an absorbing wall at the external domain. No waves are reflected and no accumulation of energy in the system will take place. Comparing the estimates in domain (2) to the findings of domain (2) in the one dimensional two domain system, see section 4.2, we find the estimates of the present system all to be smaller. This is due to the circular geometry of this system. The waves of the acoustic fields in domain (2) are distributed on an increasing area as they travel outwards. That is to say the intensity of the field is radially decreased within domain (2). A similar intensity increment of outwards propagating waves is not seen within the system in section 4.2 being one dimensional.

The findings of domain (1) is the exact same as for the one domain system considered in section 5.1.2 and will therefore not be treated further.

Chapter 6

Applications of acousto-fluidics in micro systems

The continued development of the lab-on-chip technology requires great knowledge within various scientific and technological fields. For instance producing a chip requires know-how of design and fabrication technologies. The chemical and biological processes of analysis within the micro-laboratory must be developed, understood and optimized. Moreover the flow must be controlled in order to maximize the performance of the whole lab-on-a-chip system.

Acousto-fluidics provides the fundamental theory necessary to actively control the flow. Being able to characterize and modify the acoustic fields within the system, by applying different boundary conditions, changing frequency etc., phenomenons such as acoustic radiation force and acoustic streaming can be used to enhance the separation or mixing of various particles within the fluid depending on which phenomenon dominates. In the following sections two different micromanipulation techniques of acousto-fluidics are described exploiting either acoustic radiation force or acoustic streaming.

6.1 Lipid particle separation from erythrocytes

During cardiac surgery the patient suffers from enormous loss of blood and blood conveying is therefore vital for the survival of the patient. Due to the surgery, the blood lost from the patient is polluted by i.a. lipid particles and can therefore not directly be re-injected into the blood circulation system of the patient. Hence the blood must be cleaned from lipid particles.

The lipid particles can be separated from the erythrocytes in an aqueous solution by the use of radiation force [6], [7], [8]. Compared to other separation methods, e.g. centrifugation, this non-contact separation method is gentle to the erythrocytes.

Applying an acoustic field perpendicular to the flow direction in micro chip system containing a solution of lipid particles and erythrocytes gives rise to standing waves. The

waves can be described by the first order perturbation fields similar to those derived in previous sections. Those fields are based on zero initial velocity which is also the case here, since the velocity field generated is perpendicular to the flow direction.

Tuning the frequency to match one half wavelength to the channel width, the pressure field can be modified to induce an antinode with high pressure along each of the channel walls and a node with low pressure in the center of the channel. Under the influence of the radiation force particles the the lipid particles and the erythrocytes are arranged most energetically favorable. The lipid particles have larger compressibility than the aqueous solution, i.e., the energy expenses of compressing a lipid particle is less than of compressing the solution. Reducing the overall energy of the system the lipid particles therefore gather in areas of high pressure; this is found in the antinodes. The erythrocytes have smaller compressibility than the aqueous solution and will therefore due to energy minimization accumulate in placed of minimum pressure, i.e., the pressure nodes.

Thus erythrocytes are to be found at the center of the channel and lipid particles in the vicinity of the walls, see Fig. 6.1, left, [9]. Due to the laminar flow the erythrocytes continue into a centered outlet at the end of the channel while lipid particles are led into the side outlets, see Fig. 6.1 right.

The efficiency of the separation method is above 90 %, [7], [8]. However it decreases with increasing blood concentration and increasing flow rate.

6.2 Mixing fluidics in laminar flow

Both the radiation force and acoustic streaming arising from an applied acoustic field causes particles within the fluid to move. However the motions due to the two phenomenons are different given the geometry. A research group at MIC has measured the velocity field induced by acoustic radiation force and acoustic streaming. Depending on physical parameters, such as particle size, one of the phenomenons may dominate. In Fig. 6.2, left, the acoustic radiation force dominates, trapping 5 μm beads in nodes of the pressure field. Meanwhile in Fig. 6.2, right, acoustic streaming is dominating and inducing a vortex motion upon 1 μm beads. Since the acoustic force scales with the volume of

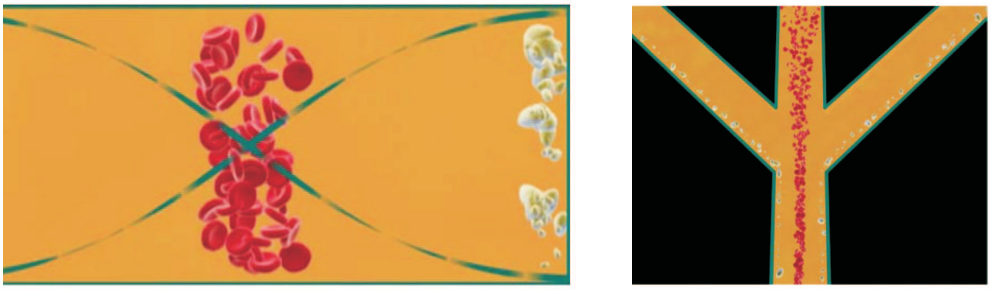

Figure 6.1: Left: Cross section of a channel. Lipid particles gather in antinodes whereas erythrocytes gather in nodes due to the acoustic radiation force. Right: The channel opens into three channels separating the lipid particles from the erythrocytes.[8]

a particle, see section 2.4.2, smaller particles are more susceptible to acoustic streaming than to the acoustic force, [9].

In lab-on-a-chip systems the flow is laminar, i.e., no turbulence, due to the small velocities. If not influenced by an external field all mixing within the fluid only happens due to diffusion. Though the distances in a micro chamber are small the diffusion is too slow to cause sufficient mixing.

Using acoustic radiation generated by an applied acoustic field, the mixing time can be decreased. This is investigated by the SMART-BioMEMS research project. [12]. Commenced in December 2005 the project is scheduled to conclude on November 2008. The project aims to develop a micro analysis system which delivers an entire genetic mutation analysis. In particular the project focuses on the detection of point mutations in gene p53 relevant e.g. for cancer development. The chip is expected to facilitate a finely detection of gene mutations and on long term add knowledge useful for the preventing of genetic diseases. Other areas such as food safety and environmental monitoring may also benefit of enhanced understanding of the human genoms.

In the SMART-BioMEMS chip the polymerase chain reaction (PCR) amplifies the DNA by splitting the helix into single strands and numerously copying the strands. Mutations are now detectable, but to ensure a correct detection result all strands must at least once during the analysis be brought in contact with the detection system. If mixing is only to rely on diffusion the duration of every analysis is excessively. The project therefore aims to reduce the mixing time using acoustic flow control.

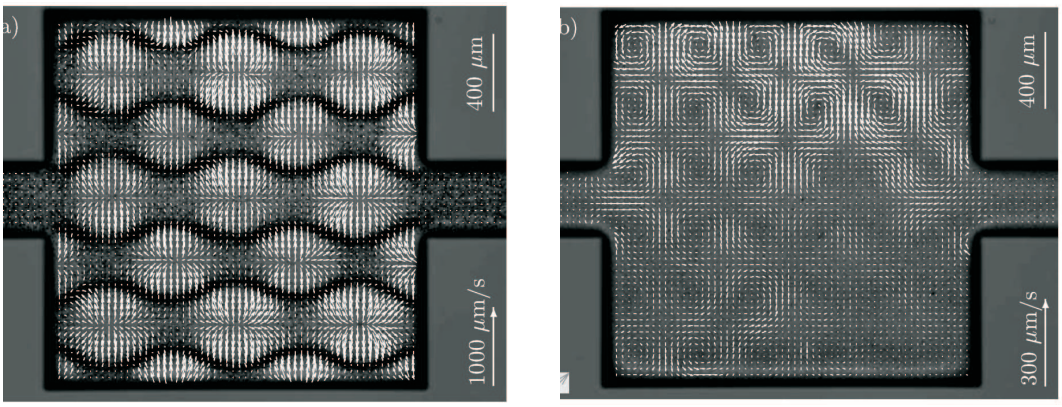

Figure 6.2: Left: Acoustic radiation force dominates for large particles. Here for 5 μm beads. Right: Acoustic streaming dominates for small particles. Here for 1 μm beads. In each of the figures the arrow placed in the lower right corner indicates the size of the velocity fields. The acoustic radiation force is seen to induce the largest velocity components.[9]

Chapter 7

Discussion

The theory concerning acoustics in microfluidic systems has been studied using perturbation calculation. Perturbation theory provides good approximative solutions to non-linear problems. By varying the order of the expansion, i.e., the number of terms to include, the method can be adjusted to suit a specific system to a certain accuracy. First order perturbation is found to sufficient to describe the acoustic fields in the case of steady state. Terms of higher order can thus be neglected leading to a simplification of the equations to be solved. However describing phenomena like acoustic streaming and radiation force requires higher orders. First order perturbation represents oscillating fields with the zero time average over a full period whereas second order perturbation yields non-oscillating fields causing a non vanishing time average. The disadvantage of perturbation expansion method is that it imposes demand of a known solution to the unperturbed system. Fortunately within this project the zeroth order solutions have been well established.

Within the use of perturbation theory the sound velocity, c_a, arises in the governing equations. For compressible fluids the sound velocity cannot be assumed to be constant unless a linear relation between pressure and density is found to exist. Unfortunately we have not found enough data to deduce whether this is the case. The given data results in the non-linear parameter $\gamma^* - 1 \simeq 7$ which definitely is too high for c_a to be presumed constant. However first order perturbation expansion is linear and therefore the non-linear parameter is only of importance when considering second order perturbation or higher order.

The presented theory has been applied on different simple geometries with various boundary conditions. The systems consist of idealized physical models. For instance we have in some of the models assumed the considered systems to be completely isolated allowing no transmission of the acoustic field to the surroundings. This assumption do not apply in real physical systems. Relating to the far more complicated actual lab-on-a-chip system the findings do therefore not give any quantitative answers. However the systems deliver an overall understanding of the emerging acoustic fields resulting in the case of resonance.

We find that the magnitudes of the acoustic fields depend mainly on the boundary conditions of the system. Having a boundary condition allowing no transmission of waves the energy provided by the piezo actuator will accumulate within the system and we see a large resonance. In contrast, enclosing the system by an absorbing wall we find the resonance to be significantly smaller as expected.

Further the geometry of the considered systems is found to be of importance for the size of the amplitude in case of resonance. Expanding the systems from one dimension to two dimensions find the intensity to decrease radially whereas it is preserved for all x in the one dimensional case. This is the physical interpretation of the Bessel functions appearing in finite circular geometries in contrast to the trigonometric functions which we find in the one dimensional cases.

To set up a realistic physical model attenuation must be included. However, comparing one dimensional systems with circular systems the findings suggest that attenuation only have an impact in the one dimensional case. Terms expressing the attenuation seems to be negligible in the equations describing the circular systems. Moreover the amplitudes of the resonance cases are finite.

This seems astonishing when expecting resonance of infinite amplitude as a result of excluding attenuation. This discrepancy between the findings and our expectations will be an interesting subject for further studies, however, this is beyond the extent of this project.

Chapter 8

Outlook

In this thesis the perturbation theory is seen to deliver useful solutions of the acoustic fields within the considered geometrical cases. However there are still areas to be studied when using second order perturbation. This comprises the sound velocity which can be perceived as constant in first order perturbation but not in second order. The reason for this is the emergence of the non-linear parameter. Suitable data is required to estimate the possibility of assuming constant sound velocity, and we leave the investigation of this area as a request for further studies.

For circular symmetric systems we found the attenuation to be insignificant. From a physical perspective this do not seem realistic and a more throughout investigating of the disagreement is an interesting subject for prospective research.

Within this project we have only studied simple systems. To gain knowledge of more complicated models a natural extension of this project is to modulate various setups using a simulation program.

Chapter 9

Conclusion

Through the preparation of this thesis the theory of acoustics in microfluidics have been studied. Using perturbation theory the first order acoustic fields have been derived and cases of resonance have been analyzed.

Overall we find the case of resonance to depend on the geometry and the set up of the boundary conditions for a specific problem. We have considered systems enclosed by a piezo actuator. This setup implies large amplitudes of the acoustic fields compared to experimental findings by others. The discrepancy arises from the undetermined amplitude of the piezo-induced acoustic field. Further we have considered systems with an absorbing wall at the outer boundary. Here we find the amplitudes of the acoustic fields more in accordance with results found by experiments.

Setting up an analytically solvable system involves simplifications and physical idealizations. Despite of their simplicity, the considered systems provide a solid foundation to the further understanding and study of far more complicated fluidic systems that is seen in lab-on-chip-systems.

Appendix A

Estimation of the non-linear parameter

In this appendix the magnitude of the non-linear parameter $\gamma^* - 1$ for water is estimated applying the data from [5]. The data is plotted in Fig. A.1 and a second order polynomial is fitted to the points. The fitting curve has the equation

$$p = 0.00635\rho^2 - 10.46536\rho + 4118.7186, \tag{A.1}$$

and thereby the first and second derivative gives

$$\frac{dp}{d\rho} = 1.27 \times 10^{-2}\rho - 10.46536, \tag{A.2}$$

$$\frac{d^2p}{d\rho^2} = 1.27 \times 10^{-2}. \tag{A.3}$$

The non-linear parameter can now be determined using Eq. (2.9)

$$\gamma^* - 1 = \frac{\rho_0(\partial_\rho^2 p)_0}{(\partial_\rho p)_0}, \tag{A.4}$$

$$= \frac{\rho_0 1.27 \times 10^{-2}}{1.27 \times 10^{-2}\rho_0 - 10.46536}, \tag{A.5}$$

$$= 5.68. \tag{A.6}$$

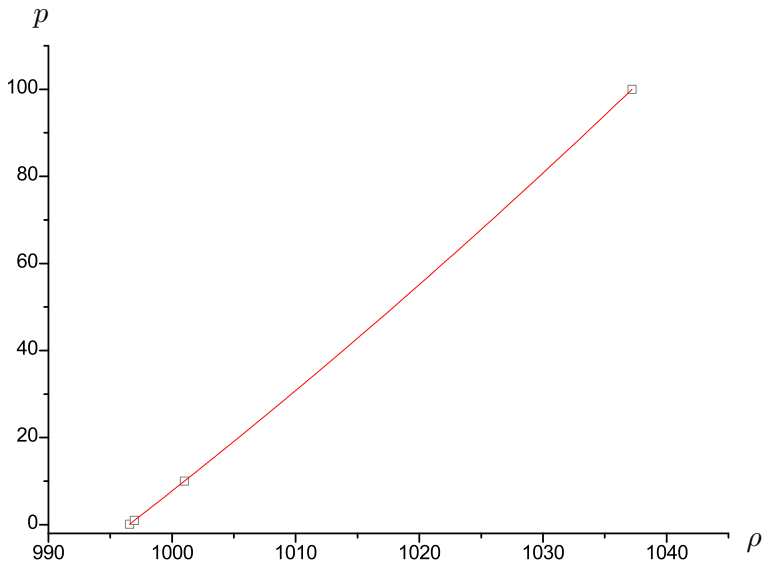

Figure A.1: The pressure p (MPa) as a function of the density ρ (kgm^{-3}) plotted from data provided from [5].

Appendix B

Useful formula

In this appendix the formula $\langle A(t)B(t)\rangle = \frac{1}{2}\mathrm{Re}[A_0 B_0^*]$ is proved.

The two considered complex functions are given by

$$A(t) = A_0 e^{-i\omega t}, \tag{B.1}$$
$$B(t) = B_0 e^{-i\omega t}, \tag{B.2}$$

where A_0 as well as B_0 may be complex. The time average then becomes

$$\begin{aligned}
\langle A(t)B(t)\rangle &= \langle \mathrm{Re}[A_0 e^{-i\omega t}]\mathrm{Re}[B_0 e^{-i\omega t}]\rangle && \text{(B.3)}\\
&= \langle \frac{1}{2}(A + A^*)\frac{1}{2}(B + B^*)\rangle && \text{(B.4)}\\
&= \frac{1}{4}\langle AB + A^*B^* + AB^* + A^*B\rangle && \text{(B.5)}\\
&= \frac{1}{4}\langle AB^* + A^*B\rangle && \text{(B.6)}\\
&= \frac{1}{2}\mathrm{Re}[A_0 B_0]. && \text{(B.7)}
\end{aligned}$$

Appendix C

Time averaging

Calculating the time average of the second order terms of $\mathbf{v}_2$ and ρ_2, the following equations are needed

$$\rho_0 \partial_t \mathbf{v}_2 = -\boldsymbol{\nabla} p_2 - \rho_1 \partial_t \mathbf{v}_1 - \rho_0 (\mathbf{v}_1 \cdot \boldsymbol{\nabla}) \mathbf{v}_1 + \eta \nabla^2 \mathbf{v}_2 + \beta \eta \boldsymbol{\nabla} (\boldsymbol{\nabla} \cdot \mathbf{v}_2), \tag{C.1}$$

$$p_2 = c_a^2 \rho_2 + \frac{1}{2} (\partial_\rho c^2)_0 \rho_1^2, \tag{C.2}$$

$$\partial_t \rho_2 = -\rho_0 \boldsymbol{\nabla} \mathbf{v}_2 - \boldsymbol{\nabla} \cdot (\rho_1 \mathbf{v}_1). \tag{C.3}$$

First the time average of $\mathbf{v}_2$ is found. Letting $\rho_2 = \rho_2^0 + A_0 e^{-2i\omega t}$, this results in $\partial_t \rho_2 = -2iA_0 \omega e^{-2i\omega t}$. Since the time derivative only depends on the second term of ρ_2 we only averages on a harmonic function which as well known has a zero time average, hence $\langle \partial_t \rho_2 \rangle = 0$. From Eq. (C.3) the time average of the velocity then becomes

$$\boldsymbol{\nabla} \langle \mathbf{v}_2 \rangle = -\frac{1}{\rho_0} \boldsymbol{\nabla} \cdot \langle (\rho_1 \mathbf{v}_1) \rangle. \tag{C.4}$$

Using this result the time average of $\nabla^2 \rho_2$ can now be evaluated. Taking the divergence of Eq. (C.1) and inserting Eq. (C.2) we get

$$\begin{aligned} \rho_0 \partial_t \boldsymbol{\nabla} \cdot \mathbf{v}_2 = &- \nabla^2 (c_a^2 \rho_2) - \frac{1}{2} (\partial_\rho c^2)_0 \nabla^2 \rho_1^2 - \boldsymbol{\nabla} \cdot (\rho_1 \partial_t \mathbf{v}_1) - \rho_0 \boldsymbol{\nabla} \cdot ((\mathbf{v}_1 \boldsymbol{\nabla}) \mathbf{v}_1) \\ &+ \eta \boldsymbol{\nabla} \cdot (\nabla^2 \mathbf{v}_2) + \beta \eta \nabla^2 (\boldsymbol{\nabla} \cdot \mathbf{v}_2). \end{aligned} \tag{C.5}$$

Determining the time average with insertion of Eq. (C.4) and again using the fact that $\langle \partial_t \mathbf{v}_2 \rangle = 0$ we find

$$0 = - c_a^2 \nabla^2 \langle \rho_2 \rangle - \frac{1}{2} (\partial_\rho c^2)_0 \nabla^2 \langle \rho_1^2 \rangle - \rho_0 \langle \boldsymbol{\nabla} \cdot (\mathbf{v}_1 \cdot \boldsymbol{\nabla}) \mathbf{v}_1 \rangle - \frac{\eta(\beta+1)}{\rho_0} \nabla^2 (\boldsymbol{\nabla} \cdot \langle \rho_1 \mathbf{v}_1 \rangle), \tag{C.6}$$

$$\begin{aligned} \nabla^2 \langle \rho_2 \rangle = &- \frac{1}{2c_a^2} (\partial_\rho c^2)_0 \nabla^2 \langle \rho_1^2 \rangle - \frac{\rho_0}{c_a^2} \boldsymbol{\nabla} \cdot \langle (\mathbf{v}_1 \cdot \boldsymbol{\nabla}) \mathbf{v}_1 \rangle + \frac{i\omega}{c_a^2} \boldsymbol{\nabla} \cdot \langle (\rho_1 \mathbf{v}_1) \rangle \\ &- \frac{\eta(\beta+1)}{c_a^2 \rho_0} \nabla^2 (\boldsymbol{\nabla} \cdot \langle \rho_1 \mathbf{v}_1 \rangle). \end{aligned} \tag{C.7}$$

Bibliography

[1] *Theoretical microfluidics*,
Henrik Bruus
Oxford University Press, **in press**, (2007).
Oxford, England.

[2] *Theory og Nonlinear Acoustics in Fluidics*,
Bengt O. Enflo and Claes M. Hedberg
Fluid mechanics and its applications. **67**, ch. 2 (2002).
The Netherlands.

[3] *Matematisk Analyse 2*,
Per W. Karlsson, Vagn Lundsgaard Hansen
Danmarks Tekniske Universitet. **1**, p. 193 (1998).
Lyngby, Danmark.

[4] *Partial Differential Equations*,
Nakhlé H. Asmar
University of Missouri, **2**, ch.4 (2005).
New Jersey, USA.

[5] *Handbook of Chemistry and Physics*,
CRC, **87**, (2006-2007).
http://www.hbcpnetbase.com.globalproxy.cvt.dk/

[6] *Non-contact micromainpulation using an ultrasonic standing wave field*,
Teruyuki Kozuka, Toru Tuziuti, Hideto Mitome and Toshio Fukuda
IEEE. (1996).

[7] *Acoustic control of suspended particles in micro fluidic chips*,
Filip Petersson, Andreas Nilsson, Henrik Jönsson and Thomas Laurell
Lab chip. **4**, (2004).

[8] *Continuous separation of lipid particles from erythrocytes by means of laminar flow and acoustic standing wave forces*,
Filip Petersson, Andreas Nilsson, Cecilia Holm, Henrik Jönsson and Thomas Laurell
Lab chip. **5**, (2005).

[9] *Acoustic resonances in microfluidic chips: full-image micro-PIV experiments and numerical simulations*,
S. M. Sundin, T. Glasdam Jensen, H. Bruus and J. P. Kutter
Lab chip. **in press**, (2007).

[10] *Acoustic radiation in microfluidic systems*,
Masterthesis
Thomas Glasdam Jensen
MIC, Techical University of Denmark. **1**, (2007).
Copgenhagen, Denmark.

[11] *wikipedia.org*
Topics: fluid mechanics,

[12] *smartbiomems.com*
SMART-BioMEMS research project